

Chapter 2

Literature Review

Abstract This chapter reviews the literature related to tactile interaction for perception of slippage and texture. The first section presents the research in psychophysics that relate to tactile perception of texture using a bare finger or through tools and devices. The next section describes the properties of the skin from a mechanical viewpoint. Both mechanical response and friction properties will be related to roughness perception and the creation of vibrations. Finally, the current state of the art in devices that reproduce virtual haptic textures is portrayed.

2.1 Human Perception of Tactual Texture

Tactual texture concerns the surface and material properties that our finger perceives by coming into contact with an object and/or sliding on the surface. The nature of surface contact is a key factor in the tactile identification of objects. It reveals mechanical properties such as friction, roughness and temperature, and informs the central nervous system about the qualities of the contact. Furthermore, this information is essential to grasping and manipulating our environment.

2.1.1 Texture Sensing

2.1.1.1 Active Touch for Perception

Motion is an intrinsic part of haptic perception. Without making contact, manipulating, or stroking an object, it is impossible to sense the shapes, textures, materials that surround us. Katz, in his classic monograph [71, 78], was the first to notice that tactile perception is intimately linked with self-motion. He hypothesized that the size of the perceptual window is augmented by moving it in the world. The motion of the finger or the hand makes the resolution and the reach of touch virtually infinite. The same observation has been also applied to visual perception, in which the movement of the eye plays a important part in scene comprehension. Katz also claimed that without relative lateral motion between an object and the skin, the roughness of

a surface cannot be estimated. Roughness is defined by micro-scale asperities of the surface; at length scale well below the spatial detection threshold of touch.

These observations have been experimentally verified by Meenes and Zigler [101] who showed that the roughness of various grades of paper is optimally perceived by moving relative to the surface. The lateral motion introduces temporal variation in the mechanical pressure applied to the skin, which is used as a cue for roughness estimation. Lederman and Klatzky [84], in a seminal article, drew a taxonomy of hand movements used for tactual perception. They found eight exploratory procedures from which humans extract information about a tangible object through of touch. Texture, for instance, is perceived through lateral motion between the object and the finger, and compliance with a variable pressure normal to the surface.

Gibson observed that vision and touch share similarities, as self-motion is necessary for perception [43]. Using simple planar shapes, he asked two groups to match their tactile sensations with drawings of the shapes. In the first group, the shapes were simply pressed into the hands of participants. The second group was free to explore the shapes and boundaries of the objects before giving an answer. The results of this experiment showed a clear advantage of exploratory motion for the perception of shapes.

As Katz noted, tactual abilities for texture discrimination are also greatly impaired by the absence of relative lateral motion. Psychophysical evaluations of human ability to discriminate coarse gratings (groove size greater than 100 μm) reveal that the discrimination thresholds drop significantly when participants are not allowed to move their finger. During this experiment, Morley et al. [108] also noticed that exploratory procedures follow an almost sinusoidal displacement of the finger from right to left. This observation can possibly be induced by the unidirectionnality of the rectangular grating.

In light of these findings, it is clear that in order to reproduce virtual surfaces, users have to be able to explore the virtual world with their hands. In particular, texture is sensed during lateral motion of the finger onto the surface.

2.1.1.2 Perceptual Dimensions

Texture is a term that encompasses many features of the surface being explored. Hollins et al. [52, 53] tried to reduce these features to a minimum number of descriptors. They performed a study in which they presented to non-expert participants a total of 17 tactile stimuli, such as sandpaper, wood, velvet, cork, and asked them to describe the sensations they felt with a set of adjectives. From these data they ran a multidimensional scaling (MDS) analysis and found that the perceptual space could be represented as a four-dimension Cartesian space. Major axes correspond to the description of roughness (smooth-rough) and compliance (hard-soft) of the material. The two minor axes are most likely to be frictional properties (sticky-slippery) and temperature (warm-cold). It is interesting to notice that the axes are not orthogonal to each other, indicating a cross-correlation between attributes.

Using a free-sorting procedure on 24 car seat fabrics, Picard et al. [131] found, also by mean of an MDS analysis, that the perceptual space could be divided in to three to four dimensions. However the major dimensions were soft/harsh and thin/thick, as opposed to previous studies. This difference might be explained by the fact that the participant were French speaker and that the words “soft” and “harsh” are more commonly referred to fabrics than “rough” and “smooth”. This result emphasis the great influence of culture and context on the cognitive classification of sensations.

The perceptual space suggested by Hollins et al. [53] was constructed around subjective attributes which depend of the context and are not always reliable. The limited number of samples must also be taken into account. In fact, 17 samples with 4 dimensions do not create enough redundancy for correct statistics. With this limitation in mind, Bergmann-Tiest and Kappers [11] performed a free sorting study with 124 texture samples. Each of the samples was classified from its mechanical properties, such as compliance (inverse of stiffness) and roughness computed from a weighted average spectrum of the height profile. The MDS procedure, they used embedded the results in a four dimensional space. The dimensions correlated with the physical measurements but they were not completely aligned, which suggests that each perceptual dimension is based on several physical properties. Furthermore, the physical attributes of roughness and compliance described a horseshoe shape in perceptual space, which contradicts the hypothesis of a Euclidean perceptual space.

When analyzing individual dimensions, Smith and Scott [141] reported that the friction coefficients (quantified as the tangential forces divided by the normal forces) was correlated with stickiness judgments on smooth surfaces. In the case of non-smooth surfaces, roughness perception also seemed to be correlated with increasing net friction (i.e., tangential force) [143]. From this viewpoint, it is clear that the continuum rough/smooth is not orthogonal with sticky/slippery. Moreover, they also found that roughness estimates were not directly correlated with topographical measurements of surface asperities. Stevens and Harris [150] performed a quantitative study of the perceived roughness of textiles with increasing emery cloth grid number; the grid number is inversely proportional to the particle diameter. They found that roughness was a positive power of grid number. They also found that smoothness varied similarly, but with opposite power, with grid number. This last result confirms that smoothness is the reciprocal of roughness. Ekman et al. [35] extended these results and found that the exponent of the power-law depends on the coefficient of friction and the material used (sandpaper, cardboard and paper).

Yoshioka et al. [185] explored the perceptual dimensions of texture explored through a rigid probe. They asked participants to rate various textures on a three dimensional space that comprised roughness, hardness and stickiness. They found no significant difference between the probe and the bare finger. The authors claimed that in the case of indirect touch, the three dimensions correspond to the vibration power transmitted by the tool, the compliance of the surface and the friction force acting on the probe during manual exploration. These results do not agree with the other studies, probably because the experimental procedure imposed the dimensions of the perceptual space a priori.

Despite discrepancy in the definition of tactual texture, all these studies corroborate the fact that texture is associated with multiple attributes in which roughness plays a fundamental role.

2.1.1.3 Differences Between Coarse and Fine Roughness Perception

Katz [71, 78] was also the first to distinguish between the perception of coarse and fine roughness. The former can be felt simply by pushing on the surface, whereas the small asperity size of fine surfaces require a lateral motion of the skin with respect to the surface in order to be perceived. Further experiments confirmed this hypothesis, by showing that without relative motion, surface defects below 100 μm in size can not be detected [51, 86, 157]. It is worth noting that these findings also showed that speed does not influence the perceptual estimation of roughness, while normal force increases roughness magnitude estimates. These observations show the independence of the roughness estimate with respect to temporal factors, and lead to imagine that roughness is represented by the central nervous system, in space rather than in time.

When a tactile signal is repeated for a long time, the human sensory system adapts and apparent amplitude decreases: when the signal is stopped, the sensitivity progressively recovers its function. Lederman et al. [87] asked participants to rate the roughness of coarse textured surfaces before and after inhibiting vibrotactile sensitivity with high and low frequency masking stimuli. No change in the perception of coarse textures was observed suggesting that the perception of coarse textures is not mediated by vibration. Later, Hollins et al. [51] performed the same experiment, using fine textures and found a significant decrease in discrimination abilities following adaptation to high-frequency stimuli. The results of both studies can be interpreted by supporting a *duplex theory* of roughness perception; large asperities of roughness are perceived as spatial determinants, whereas fine textures ($<200\ \mu\text{m}$ of spatial frequency) are mainly perceived through temporal determinants, consisting in vibrations created by sliding friction between the textured surface and the finger. Moreover, vibrations are both necessary and sufficient for the perception of fine textures [55].

From the literature on texture perception, we can conclude that tactual perception of roughness is based on a combination of two perceptual cues: the spatial and temporal determinants. The first category relates to the deformation pattern of the skin in contact with a surface, and is dominant when surface defects are coarse. Temporal determinants are produced by the time-varying global deformation of the skin, which is excited during lateral motion between the skin and texture, and they prevail when texture is fine (i.e., $<100\ \mu\text{m}$ of height). Both of these cues are involved in the tactual perception of surface topography and friction properties. Depending on the mechanical events, the central nervous system will rely on one or the other cue.

2.1.1.4 Perception Through a Rigid Link Compared to Bare Finger Exploration

The central nervous system has the capability of extending the function of the body via the tools we hold. For instance when we are using a pen to write, the pen is integrated in our sensory system, and our mind controls the tip of the pencil rather than managing the forces and torques on the body of the tool. This is also true for tactual perception: a stick stroked on a rough surface transmits vibrations that one captures by the mechanoreceptors in the hand. But from a physiological point of view, the mechanical deformation field that mechanoreceptors embedded in the skin sense is only the pressure of the skin on the surface of the pen. So how does the central nervous system interpret the vibratory signal from the stick as being comparable the bare finger exploration?

Klatzky and Lederman [75] compared roughness judgments when subjects explored textured surfaces with a rigid probe or a rigid sheath mounted on their fingertip with judgements made when exploring with the bare finger or through a compliant glove. In the first condition, the rigid link imposes a coding of tactual perception based on vibration alone, whereas the bare finger condition gives access to both vibratory and spatial cues. The authors report that roughness estimates were greater with a rigid link. Discrimination performance was best with the bare finger, but the rigid sheath only reduced discrimination by few percent. This experiment shows the importance of vibratory cues during texture exploration. One explanation for the greater subjective magnitude when using a rigid link is that the finger and the compliant glove serve to damp the vibration content. On the other hand, the rigid link amplifies vibrations produced through collisions with edges of the surface.

In [88], the same authors investigated the influence of speed and mode of touch during tactile exploration with a probe. In the passive mode, participant's arm was attached to a table while a robot stroked sandpapers on the tip of the probe they were holding. In the active mode, subjects explored sandpaper by actively stroking the probe. The resulting data showed that speed has a larger effect during passive exploration. The authors argued that because kinesthetic information from the arm motion was absent, subjects relied on cutaneous cues to assess both speed and roughness. However, a conflict is involved, because estimating the speed of motion without kinesthetic feedback relies mostly on texture information. Changing the texture reference changes the distribution of frequency content, and biases hence biased the speed or the roughness estimate. In another publication, they also explored the effect of a rigid sheath superimposed on the fingertip on tactile perception [85]. Orientation and compliance discrimination were greatly reduced by the absence of distributed spatial information. Roughness estimates and vibrotactile sensitivity were, however, less affected by spatial masking. This supports the difference between spatial and temporal determinants and their importance to tactile perception in everyday life.

The work of Yoshioka et al. [185], presented in Sect. 2.1.1.2, also showed that the subjective scaling of texture stimuli on the roughness, hardness, and stickiness continua in probe condition are similar but not identical to the bare finger exploration

mode. The cognitive classification of texture is analogous despite the difference in the mechanical signals sensed by the central nervous system in the two modes of exploration. The conclusion of this study was that the cognitive mechanisms implicated in texture perception differ for probe versus bare finger exploration. In the case of exploration with a probe, texture is reconstructed depending on the tool that participants are holding.

2.1.2 Texture and Slip Discrimination

Human capabilities of surface feature discrimination (periodic or non-periodic) have been intensively studied using psychophysical methods. Psychophysics is a branch of experimental psychology that relates perception and physical stimuli. In practice this leads to the study of verbal responses given by participants when they are stimulated in a controlled manner. Knowledge about the inputs and outputs of the human sensory system makes it possible to extrapolate its behavior. In practice, an emphasis is placed on measuring the lowest stimulus that triggers a reaction (absolute threshold) or the lowest difference of stimuli that triggers a response (difference threshold¹) of human perception.

2.1.2.1 Texture

Johansson and LaMotte [62] determined the detection threshold of the height of a single defect in a perfectly smooth silicone wafer. They found that an edge as high as $0.85\text{ }\mu\text{m}$ could produce a sensation. Raised dot detection thresholds were determined to be 1.09, 2.94 and $5.97\text{ }\mu\text{m}$ for dots of respective diameters 602, 231 and $40\text{ }\mu\text{m}$. Detection thresholds depend on the area of stimulation and, by extension, the number of receptors involved. Several studies have used raised dot matrices [80] or linear gratings [69, 108, 114] to study the effect of repetitive texture discrimination. For instance, Miyaoka et al. [106] used aluminum-oxide abrasive paper of varying grit, corresponding to average particle sizes of 40 to $1\text{ }\mu\text{m}$. They determined that the smallest perceptible difference (difference threshold) in grit was about $2.4\text{ }\mu\text{m}$.

The main criticism of these studies is that they were conducted with non-smooth topographical function, yielding gratings or surfaces that contain sharp edges and corners that can induce strong shocks and call to question the influence of height in the detection threshold. Louw et al. [91] considered the detection problem using a set of Gaussian bump profiles with a wide range of width ($0.15 < \sigma < 240\text{ mm}$). Participants were able to freely explore samples with their bare fingers. The minimum detectable height of the bump was about $1\text{ }\mu\text{m}$, on average for the smallest

¹The difference threshold relative to the stimulus intensity is called Weber fraction in honor of one of the founders of psychophysics: Ernst Heinrich Weber (1795–1878).

bump width. This value is about 10 times smaller than the size of skin cells themselves, raising questions about the physical limits of haptic perception. When the results were plotted on a log-log scale, they were linearly aligned, such that the amplitude threshold depended on the width σ raised to the power 1.3. The maximum value of the first derivative of height (maximum slope) is the dominant perceptual cue for shape and texture perception.

Building on these observations, Nefs et al. [115] used sinusoidal gratings to explore perceivers ability to discriminate amplitude and spatial frequency with periodic and mathematically defined surfaces. They found the Weber fraction for amplitude discrimination to be about 10 to 15 % which yields a difference threshold as low as 2 μm . The difference threshold for spatial period discrimination is about 11.8, 6.3 and 6.4 % for gratings of spatial period of 10, 5 and 2.5 mm respectively. Spatial discrimination thresholds were higher than values found in [108], probably because the latter authors used a continuous function for the grating shape. Conversely, the study of Morley et al. used gratings with sharp edges, so that collisions between the finger and texture corners might have created mechanical events that were easily sensed by the human sensory system.

The extremely high tactile sensitivity to surface defects is, as mentioned earlier, surprising. In quasi-static settings, the tactile sensory system can barely discriminate two dots less than 0.5 mm apart [69], but the dynamic interaction results in a hundred-fold increase in spatial sensitivity. It seems that this capability is not attributed to quasi-static sensory capabilities, but instead to the integration of mechanical signals felt during motion. In fact, the mechanical discrimination threshold in quasi-static conditions² and the roughness estimate during active touch are not correlated [90]. It confirms the idea that the central nervous system uses special strategies to perceive fine textures. Thanks to this effort, even with relatively scattered mechanoreceptors, the central nervous system is able to access sub-micrometric geometries.

Looking at the mechanical forces generated during active touch also gives some insight into the interaction between the surface and the finger. Smith et al. [142] measured tangential and normal forces (referred in this manuscript as F_t and F_n respectively) that arise from the friction between a finger and a non-smooth surface. Surprisingly, they found no effect of normal force on subjective scaling of the roughness. However the derivative of the tangential force (dF_t/dt) is highly correlated with roughness estimates. Moreover the net friction force (average of the tangential force) is also a factor in perception. Authors hypothesized that the central nervous system assesses the roughness by comparing the root mean square of variation of the tangential force with the net friction coefficient. Therefore a lower friction force, achieved by lubricating for instance, results in a lower roughness estimate with the same surface pattern.

²The spatial discrimination threshold is also known as the two-points discrimination threshold.

2.1.2.2 Slip and Velocity Perception

The awareness of slipping and the estimation of relative speed are crucial for day-to-day manual interaction. Interacting with our environment involves grasping and manipulating objects. Cutaneous information about the mechanical properties of objects helps to accomplish these tasks correctly [19, 176]. The reader can find more details about the role of cutaneous perception in precision grasping tasks in the literature [179].

Texture and slip sensations are intimately linked in human perception. To demonstrate this fact, Srinivasan et al. [147] used a perfectly smooth glass substrate stroked under a static finger. In the absence of defect on the surface, participants were not able to detect steady slip. However, a single 4 μm -high asperity on the surface was enough for participants to detect relative motion. Discrimination of the magnitude of relative velocity between the moving object and the finger is poor. Essick et al. [36] found that brushing the arm at different velocity yields to the Weber fraction is about 25 % and the scaling between actual velocity v_a and perceived one v_p is well described by $v_p \propto v_a^{0.6}$. The last results have been determined using a stimulus that had a limited duration, and therefore the actual speed could have been determined by either speed or duration. Depeault et al. [32] experimented with textured drum rotating under participants' skin and found a relation closer to $v_p \propto v_a^{1.1}$. They explained the discrepancy with the results of Essick et al. by the presence of a fixed duration of stimuli and participant could not rely on time to assess the velocity. They also explored the effect of various textures on speed judgement, and it appeared that speed estimates are varying with spatial period. One explanation is that speed is temporally encoded relative to a spatial texture, when the finger is static. Therefore, if the speed v doubles and at the same time the spatial period λ is also doubled, the temporal frequency f remains the same ($f = v/\lambda$). In this experiment the finger was stationary, so that the velocity estimate was based only on tactile information. In active perception the somatosensory system integrates the motion of the limb to make an estimate of speed. Moreover, the texture was fine, so the central nervous system can be assumed to exclusively base its estimate temporal frequency content. It is interesting to note that the reciprocal is not true; roughness estimate was independent of scanning speed [102].

Contrary to steady slip, the initial transition between stick and slip is a mechanical event perceptible even in absence of asperities on the surface [147]. This rapid transition creates vibrations that are felt by the sensory system and exploited by the central nervous system to evaluate the slipperiness and the roughness of the contacting surface [64]. This initial slip provides sufficient information for the central nervous system to be able to assess the friction coefficients of the material and to adjust the normal force accordingly [141]. Moreover the direction of slippage seems to be given by the direction of the tangential force applied on the finger during sliding [107].

In conclusion, relative velocity and slippage are key pieces of information for object identification, but are also crucial for grasp and manipulation. The central nervous system develops a number of strategies to evaluate these cues, and in both

cases texture plays a determinant role. Sliding motion on a surface gives rise to mechanical vibrations that excite the human sensory system and that are used to assess contact conditions. If slippage is imminent, the body shape and muscle tonus are adjusted to avoid dropping the object. Evidence also shows that information about slip and texture is contained in variation of the tangential force over time. The net tangential force vector during incipient slip or sliding is also a primary indicator of slipperiness. The norm of the tangential force is correlated with stickiness and the friction properties of surface being touched. The direction of this vector also gives information useful for grasp stability, for instance, and sliding direction.

2.1.3 Mechanotransduction

The fovea of the retina and the fingertip share much in common, despite their numerous differences [187]. Both are two-dimensional tissues that comprise a dense population of receptors creating zones of high acuity [69]. Fingertips, which are covered by glabrous skin, embed mechanoreceptors near the surface of the skin. These cells have the property to transduce mechanical disturbances, such as pressure and vibration, into action potentials that are transmitted to the central nervous system through the nerves. Different type of mechanoreceptors populate hairy and glabrous skin, although some types are present in both. The present review is limited to receptors that are sensitive to mechanical stimulation and that are present in the hand and the glabrous skin. The reader can find additional information about the mechanisms of sensory transduction in recent literature [31].

Most of these receptors are sub-millimeter in scale and their behavior is inferred from anatomical observations and electrophysiology. The former have revealed the existence of four types of mechanoreceptors in the glabrous skin. All of them are connected to myelinated nerve endings that transmit the electrical impulses to the brain. The latter has enabled researchers to probe ulnar and median nerves that run in the arms, and to directly record the action potentials thanks to a probe clamped on the outer of the nerve fiber. The capture of electrical signals during mechanical stimulation of the skin reveals four types of afferent messages. They are classified according to two attributes: the speed of adaptation to mechanical events (*slowly adaptive* SA and *rapidly adaptive* RA) and the size and the sharpness of their receptive field (type I for small receptive field with sharp edges and II for large and blurry bounded field). By habit, RA I afferents are named simply RA and type II are called PC from their well identified connections with Pacinian corpuscles.

2.1.3.1 Merkel Complex and SA Type I Afferents

Merkel nerve endings are SA I nerve afferents branching into multiple neurites that terminates in the vicinity of Merkel disks located on the boundary between the dermis and hypodermis. This boundary is undulated and the Merkel disks are located

at the tip of each undulation. They are distributed widely in the glabrous skin, and the afferent density can reach 100 per cm^2 at the fingertip [67]. Each nerve afferent branches into up to 90 fibers with two possible architectures. Some of the branches are clustered around one region and others are distributed along long chain that can reach 200 μm of length. There is still a debate about the role of the Merkel disks and their contribution to mechanotransduction [49].

SA I afferents exhibit a discharge rate that is linear with the indentation depth of a square punch, as observed in experiments with primates [14], and explained by a power law of exponent 0.7 in humans [76]. They are known to be sensitive to spatial features, and are especially responsible for the perception of edges [130], curvature [47] and coarse texture [25, 68, 134]. When scanning coarse gratings with the skin, a population of SA I afferents responds to the spatial frequency of the grating independently of speed, suggesting a spatial encoding of the stimulus [46]. Gabor filters convolved with the spatial pattern of the surface are able to predict the neural code of the SA I afferents [25]. Even though the code is mainly spatial, dynamic touch increases the sensitivity of SA I afferents by a factor of ten. Moreover, the firing pattern is not affected by velocity [70]. SA I nerves respond to a sinusoidal motion of the skin increasing in frequency by a decrease of the number of impulses by second, which makes them insensitive to vibration [92].

The spatial sensitivity of SA I afferents and their poor temporal resolution evidence the dual theory of texture perception. Coarse textures are most likely represented by SA I afferents which respond to the edges and curvatures of the surface. Fine texture perception, however, is probably mediated by rapidly adaptive afferents, which are more sensitive to vibrations.

2.1.3.2 Ruffini Endings and SA Type II Afferents

The role of Ruffini receptors is obscure. It was previously associated with SA II afferents [23], but their contribution has been recently put into question [121]. Only one Ruffini corpuscle has been found in the skin of the index finger using immunofluorescence despite, the fact that SA II afferents account for 15 % of all afferents in the median nerve [63]. However, SA II afferents are clearly associated with lateral stretch of the skin, and they respond to the lateral force during the incipient slip period. They also contribute to the proprioception of the hand (with Golgi tendon organs and muscle spindle receptors) by responding to the strain of the skin on the finger, thus giving an indication of finger position.

Some Ruffini-like structure connected to SA II afferents have been found at the frontier between the skin and the nail. These last afferents are correlated with large scale tangential force direction and amplitude on the fingertip [13]. They could be responsible for the sensation of stickiness during texture exploration as it has been shown that human sensory system relies on tangential forces cues for assessing the friction [141].

2.1.3.3 Meissner Corpuscles and RA Afferents

Meissner corpuscles are found in the glabrous skin, located at the interface on the dermis and the epidermis, as in the case of Merkel cells. But, unlike the latter, they are found in the grooves of ridges, and therefore are closer to the surface of the skin. They are composed of stacks of Schwann cells entangled with unmyelinated axon afferents. Conjunctive tissues link the stack to the boundary of the epidermal ridges that is supposed to act as a lever and amplify deformation of the ridges. For a detailed description see [120].

These anatomical properties (proximity to the surface and lever-like arrangement) are probably the explanation for the ultra-low threshold of RA afferents to transient mechanical deformation of the skin. In fact, a single 2 μm high dot moving under the skin is enough to stretch the papillary ridges and activate action potentials [82, 147].

These mechanoreceptors are found on each side of the fingerprint ridges. In glabrous skin the density can reach 1.5 afferents per mm^2 . They respond to stimuli within a radius of 3 to 5 mm, which corresponds to a receptive field five time larger than SA I afferents. However, their sensitivity is about four times higher than for SA I afferents [67]. These properties, combined with the fact that they are insensitive to static stimulation, make them ideal candidates for the perception of slip and micro slip that can occur when lifting an object [64]. They are believed to be the source of the reflex that regulates grip force to avoid the slipping of a grasped object. See [179] for a review of tactile contribution to the control of grasp.

RA afferents respond to vibrotactile stimulation between 8 and 64 Hz [65, 110]. At high amplitude, their response is similar to that of the PC which could explain humans' high sensitivity to vibration. Nevertheless, their role in fine texture perception is not clear. Adaptation to a 10 Hz vibrotactile signal, targeted to lower the sensitivity of both SA I and RA afferents, does not reduce fine texture estimate [54]. This result implies that they are not determinant in the perception of fine texture but more specialized for transient mechanical event like slippage.

2.1.3.4 Pacinian Corpuscles and PC Afferents

Pacinian corpuscles are found more deeply in the dermis. They are ovoid-shaped cells composed of about thirty concentric lamellae separated by fluid. The inner core of each corpuscle is connected to a single myelinated PC nerve [7]. The size of the all corpuscles is, on average, 1 mm long and can reach 4 mm in humans. There are about 350 of these corpuscles in the index finger and 800 in the palm [70]. Their size has made them the most studied mechanoreceptor.

This receptor is the most sensitive of all types. Pacinian channels can resolve skin displacement of 40 nm at their peak of sensitivity. This value falls down to 3 nm when the corpuscle is directly excited during in vitro studies [7]. They are effective in a frequency bandwidth from 40 Hz to 1 kHz and exhibit a U-shape sensitivity curve tuned to 250 Hz [65, 154, 167]. Between 60 and 250 Hz their sensitivity to

vibration increases at a rate of 40 dB per decade, suggesting that the Pacinian system is sensitive to acceleration of the skin [15]. Despite their spectacular temporal resolution, their spatial acuity is low to non-existent, as PC afferents account for stimulation in a large area such as a finger phalanx [63].

The high sensibility to vibration makes them the major contributor of hand-held tools perception. When holding a probe, vibrations and shocks induced by the contact of the tip with a surface are transmitted to the hand over large skin areas. Vibration of a tool which act perpendicular to the skin are best perceived than tangential ones [17].

It is believed that Pacinian corpuscles have a key role in the perception of fine texture with the bare finger. Using the aftereffect of vibration exposure at 250 Hz to suppress PC afferent responses, Hollins and colleagues [54] observed a significant decrease in the discrimination and the perceptual scaling of fine textured sandpapers. Moreover, Gescheider et al. [42] found that a 250 Hz adaptation did not impair estimates of millimeter-scale raised cones but the shapes did feel smoother. This implies that the PC afferents are responsible for the mechanical effect created by sharp transitions of the truncated cones and the fine background roughness. Also, PC channels are more sensitive to repetitive events. In fact a single dot on a smooth surface triggers mostly RA and SA I afferents whereas a sine-wave grating of 60 nm amplitude moving under the fingerpad triggers action potentials in the PC channel [82].

2.1.4 Vibration Sensitivity

The previous paragraphs showed the importance of vibration transmission and perception in the tactual exploration of textures and how it is mediated via mechanoreceptors. The present paragraph reviews the abilities of the human somatosensory system to discriminate vibrations that differ in amplitude, frequency and waveform.

2.1.4.1 Amplitude Discrimination

Vibrotactile sensitivity shares many properties with audition. For instance, the detection threshold of a sinusoidal displacement of the skin is not identical for all stimulation frequencies. The bandwidth over which the tactile system can detect vibration ranges from 0.4 Hz to 700 Hz. The typical sensitivity curve is considered to be almost flat from 0.4 to 3 Hz with a threshold at 30 μm . The threshold decreases at a rate of -16 dB per decade (or -5 dB/oct) from 3 to 60 Hz. Sensitivity in the 60–700 Hz band follows a U-shaped curve with a minimum at 250 Hz and the smallest threshold at 0.1 μm . The left part of the U-shaped curve decreases at the rate of -40 dB per decade [15].

The Weber fraction for amplitude discrimination above the perceptual threshold is about 50 % for 10 dB SL³ and decreases to 5 % at 40 dB SL [41]. It is worth noting that this variation of the perceptual threshold constitutes proof that Weber's law does not hold for all amplitude levels. Varying waveform and frequency did not improve the human discrimination ability. Similar Weber fractions were found for 25 Hz pure tone, 250 Hz sinusoid and broadband noise. This independence to signal properties suggests that the magnitude estimates are based on the relative energy of the signal.

Verrillo et al. [170] measured the curve for identical sensation in a 25–700 Hz frequency band and found these isocurves to scale in proportion to incremental amplitude, expressed in decibels, which means that it is logarithmic with the power of the signal. The only exception was for large amplitudes (>30 dB SL) and high frequencies (100–700 Hz) where the U-shape tend to flatten. The amplitude estimate for each frequency was well explained by a power law with a coefficient of 0.89 up to 350 Hz. The exponent increases with the frequency after 350 Hz.

Several conditions influence perceptual thresholds. The area of the contact is one of these factors. The aforementioned measurements were made with a 500 mm² contactor. Decreasing the area of contact caused the threshold to decrease until it reached a plateau at 30 μ m for areas below 1 mm². The accepted explanation is that small contractor areas stimulate only the surface of the skin, whereas larger contact areas transmit vibration deeper, thus excite the Pacinian channel [168]. The presence of a surround around the vibrating probe is also a factor as it blocks wave propagation and eliminates the possibility of spatial summation [166]. The temperature also affects the discrimination. At 15 °C the threshold is three time lower than at 35 °C then it stabilizes until 40 °C [169]. Lastly, thresholds are slightly different when holding a tube [17], a pen [59] or a sphere [60], but the curves of frequency sensitivity nonetheless possess the same shapes.

2.1.4.2 Temporal and Frequency Discrimination

Mahns et al. [96] measured frequency discrimination for four frequencies (20, 50, 100 and 200 Hz) when stimulating the glabrous and the hairy skin. They found the Weber fraction $\Delta f/f$ to vary from 36 % to 14 % for reference frequencies f of 20 Hz and 200 Hz respectively, when the fingertip is stimulated. Detection thresholds are substantially higher in the hairy skin, probably because of the dynamics of the skin and the fact that Pacinian corpuscles are located deeper in the hairy skin than in the glabrous skin. Other studies have found Weber fractions as low as 6 % [45, 81] for low frequency (30–40 Hz) stimulation of the fingertip.

As in audition, differences between combinations of two pure sinusoidal signals with different phase are not always well perceived [10]. Phase difference is an important feature as two signals combined with different phase delay give rise to a

³Decibel above the sensation level.

variety of different waveforms. In the case of vibrotactile sensitivity, low frequency signals (10 Hz + 30 Hz) with four different phases (0 to 270° by 90° steps) are well discriminated. At high frequencies, however, the discrimination of phase differences in comparison of combinations of two vibrotactile stimuli (100 Hz + 300 Hz) is poor. Previous adaptation to a 10 Hz signal decreases phase discrimination abilities at high frequency, even further. An explanation given by the authors is that the PC channel integrates the energy of the signal over time, and therefore has a weaker temporal consistency. Low frequencies however are mediated by the RA channel, which encodes the complex waveforms and responds with more accurate temporal resolution.

Also, concerning temporal resolution, the somatosensory system can resolve stimuli separated by 10 ms. Below this value, both stimuli are felt as one [123].

To conclude this review of the perceptual and physiological literature on touch, it seems that during bare finger exploration of textures, the human sensory system acts in a peculiar fashion. A net friction estimate is correlated with the lateral force that shears the fingertip, as possibly mediated by SA II afferents. Fine texture, however, does not depend on spatial deformation of the finger but instead on vibrations generated by the sliding motion of the finger on the surface. The Pacinian channel is a candidate for the mediation of fine texture, despite the fact that the contribution of RA afferents is possible. Finally, roughness appears to be conveyed through rapid lateral displacement of the skin and via the normal force that the finger applies to the surface has a minor influence. Hence to reproduce fine texture for the fingertip, one should, arguably, focus on variations of lateral displacement. Figure 2.1 summarize some attributes of mechanotransduction during sliding of a finger on a textures surface.

2.2 Bio-tribology of the Skin

Mechanical waves, from which the central nervous system interprets the sensation of roughness and texture, originate from friction between the skin and the surface. Sliding motion creates acoustic energy that is radiated both in the tissues and in the surrounding environment [2]. This section explores the complex structure of the fingertip, the behavior of the skin and the relation between the production of friction and vibration during tactual exploration of texture.

2.2.1 Fingertip Anatomy

Touch sensation is present everywhere on the surface of the body thanks to the innervation of our skin. But during dextrous tasks, it is the hand, and especially the fingertips, that are the most engaged. Tactual perception is also often realized by stroking, tapping or pinching the surface with the tip of a finger. Fingertips are shaped in a specific way that provides compliance and at the same time high strength. In essence,

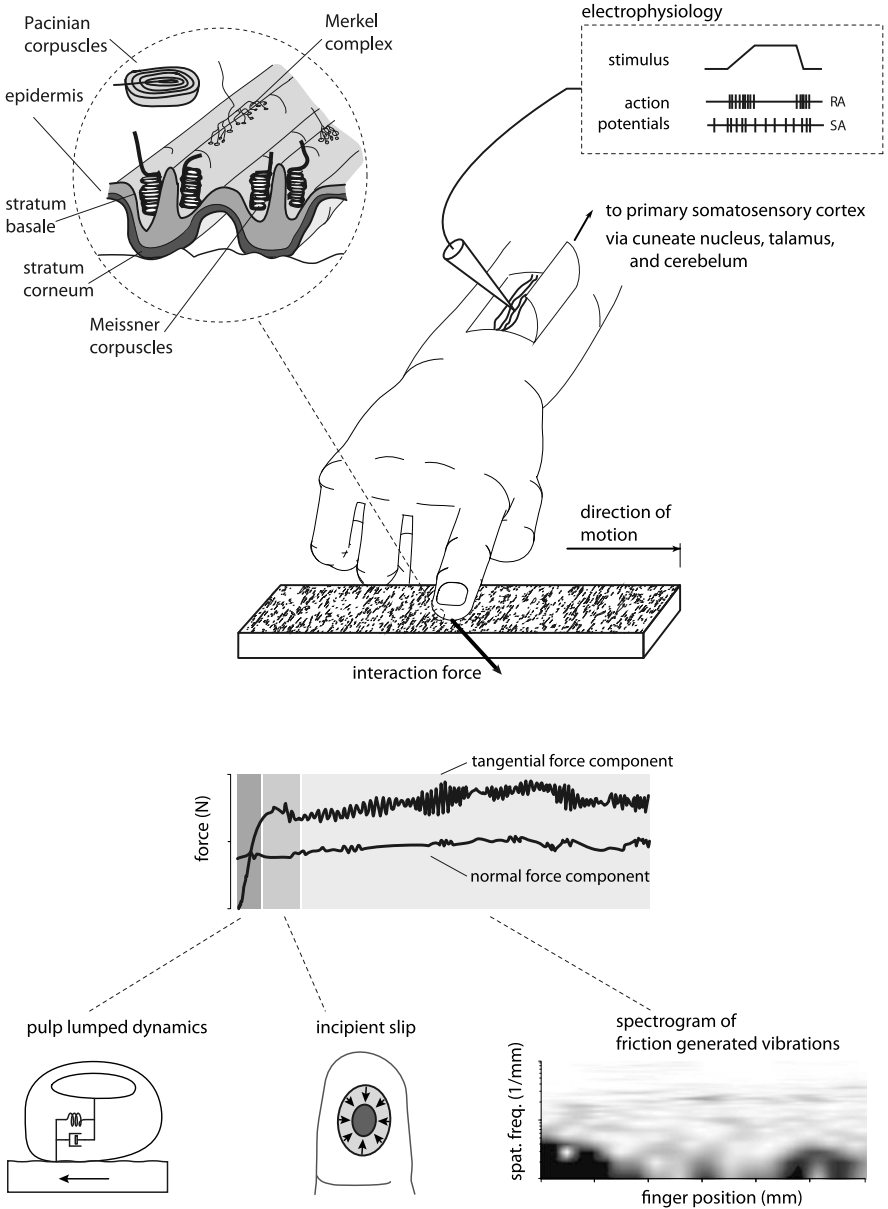


Fig. 2.1 Summary of the touch perception. Includes mechanoreceptors location (*top left*), afferents responses (*top right*), and mechanical interaction during tactual exploration (*bottom*). Inspired from [4, 65, 113, 120, 179]

the fingertip is composed of three different media. The first medium is the bone, which combine rigidity with light weight. It is connected to muscles in the forearm by ligaments fixed on each side of the bone. A rough cap terminates the bone, where collagen fibers link the skin with the tip.

These collagen fibers in the subcutaneous tissues (or *hypodermis*) create a matrix with the fat, and constitute the intermediate layer of the fingertip. This composite material can endure large deformations without breaking and is responsible for the compliance of the fingerpad. Numerous blood vessels irrigate this region and the best evidence of the blood flow can be seen when pushing of the fingertip. The color changes due to the reduction of the blood irrigation.

The last medium is the glabrous skin, which covers the volar part of the hand. The skin is composed of many layers, from the *dermis*, where the Pacinian corpuscles are lodged, to the *stratum corneum* (outer layer of the *epidermis*). Merkel cells and Meissner corpuscles are located in the curvy *stratum basale* layer which is at the boundary between the *dermis* and the *epidermis*. Finally, the *stratum corneum* is the outer layer that is in contact with the environment. It is from 10 μm to 40 μm thick and composed of dead epithelia. It is 20 to 30 times thicker on the volar part of the hand, because of the frequency of contact. Its mechanical behavior is crucial for understanding the friction properties of the glabrous skin.

On the other side of the fingertip, the fingernail is directly connected to the bone through a dense array of collagen fibers. This arrangement provides a stiff connection between the bone and the nail [138], therefore represents a good location for measuring the average position of the fingertip.

2.2.2 Mechanical Behavior of the Fingertip

The fingertip has been the subject of extensive research, and its mechanical properties continue to fascinate scientists. This section reviews the mechanical properties of the fingertip and the skin.

2.2.2.1 Bulk Viscoelastic Properties

Pawluk and Howe studied the reaction of the finger to a normal contact with a rigid planar surface [126, 127]. The pulp can be geometrically approximated by an hemisphere, however it does not adhere to linear Hertzian deformation theory during indentation. In fact, the complex structure of the tissues is probably responsible for the mechanical behavior of the fingertip during normal compression. The stiffness $K_n = dF_n/dx$ (dF_n is an increment of force and dx the displacement) of the contact linearly increases with the force. This results in an exponential form for the force-displacement curve when measured in quasi-static conditions:

$$K_n = \frac{dF_n}{dx} = aF_n + b \quad \text{and} \quad F_n = \frac{b}{a}(e^{(x-x_0)} - 1) \quad (2.1)$$

where x_0 is the initial position for which the force is null. The force is 0.3 N at 1 mm indentation and 1.8 N at 1.5 mm, which correspond to stiffnesses of 1 N m^{-1} and 4 N m^{-1} respectively. The authors also measured the distribution of pressure, and modeled it as a Gaussian curve whose center pressure reaches 30 kPa for a force of 2 N. During these indentations, the global volume was determined to be reduced by 1 %, which makes the assumption of incompressibility acceptable [148].

The pulp is also viscoelastic. One of the effect of the viscoelasticity is that increasing of the rate of pulp compression results in a stiffer reaction of the fingertip. At a indentation speed of 80 m s^{-1} the stiffness is 4 times higher than at 0.2 m s^{-1} . The viscoelasticity is also visible when the pulp is rapidly indented to a fixed value. Immediately after the indentation, the force returned by the pulp relaxes across time. The relaxation response time is composed of three decays with time constants 4 ms, 70 ms and 1.4 s. This viscoelastic behavior probably protects the fingertip against shocks by stiffening the pulp and dissipating the contact energy. The relaxation function $G(t)$ is often modeled by a sum of decaying exponential. The resulting force of the viscoelastic model $P(t)$ to an arbitrary displacement is then described by the following convolution

$$P(t) = \int_{-\infty}^{\infty} G(t - \tau) \frac{\partial F_n(x(\tau))}{\partial x} \frac{\partial x(\tau)}{\partial \tau} d\tau \quad (2.2)$$

During tapping, the finger displays a hysteresis effect that dissipates 80 % of the entry energy [136]. The non-linear viscoelastic model described by (2.2) successfully predicts the mechanical reaction resulting from voluntary tapping on flat surfaces [61].

The lateral deformation of the fingertip demonstrates similar mechanical behavior to that of normal indenting. It exhibits hysteresic losses and non-linear relaxation behavior. However the quasi-static force is linear with the lateral displacement for tangential forces up to 5 N [125]. At low frequencies, Nakazawa et al. [113] identified the fingertip in lateral deformation as a Kelvin model corresponding to a spring connected with a damper in parallel. The properties of the pulp vary with many parameters such as the normal force and also change from person to person. Stiffness values range from 0.5 N m^{-1} to 3 N m^{-1} .

For the whole finger, linear lumped element models are sufficient to describe the mechanical impedance for rapid transients [48]. The parameters are a mass of 6 to 8 g, a damping in a range of 2 and $5 \text{ N m}^{-1} \text{ s}$ and a stiffness that evolves linearly with muscle activation from 0.2 N m^{-1} to 3 N m^{-1} . The difference between the fingertip alone and the whole finger is attributed to the joint which contributes added flexibility and greater moving mass.

2.2.2.2 Local Deformation

The high deformability of the fingertip also facilitates establishing large contact areas between the skin and the object being touched even with low forces. Pushing on a flat surface with a force of 1 N results in an area of contact 60 % as large as the

value that is reached when pushing with a force of 10 N [4, 137, 144]. The friction of the skin directly depends of the area of contact between, and the large contact area enables easier control of the grip force.

The deformability of the skin is also a key factor in the large compliance of the fingertip. Measurements have shown that shearing the skin can lead to 100 % of deformation without any damage, yet the Young's modulus remains relatively high ≈ 1 MPa [172]. During lateral motion, a single bump on the surface can yield a skin stretch larger than 30 % [89].

The response to vibration seems to be bimodal. At low frequency, normal indentation with a probe is in phase with the displacement of the probe, but above 100 Hz the probe starts to decouple which implies that the tissue response is delayed by viscosity [24]. Surface mechanical waves can travel relatively long distance, at a speed of approximately 1.6 ms^{-1} [44]. The amplitude of the waves decays with the square of the distance of stimulation, which results in a decrease of one third at a distance of 50 mm. This may assist with sensing fine textures, as the vibrations are transduced by Pacinian corpuscles along the course of waves propagation [30].

2.2.2.3 Models

The observations of the fingertip reaction to various load described in the previous paragraph, have been the foundation of lumped parameters models of the fingertip. These models are usually valid for only one load distribution and do not extend easily to other boundary conditions. Moreover, they do not give any details about the stress distribution inside the tissues. This section reviews the continuum mechanics models that attempted to explain the diffusion of stress inside the fingertip and link the strain pattern to the spatio-temporal tactile perception.

A number of models are based on Boussinesq's equation for the deformation of an infinite plane and consider only the superficial layer of the skin. They also approximate the skin as a plane by unrolling the fingertip. With a simple elastic model it is possible to predict the firing rate of SA I afferents, which are sensitive to spatial determinant [37, 130]. The addition of viscosity in the definition of the material makes this model more realistic, enabling it to predict the spatiotemporal sensitivity of RA and PC afferents [165]. However, the linear slab model combined with Hertz contact does not correctly predict the non-linear behavior of the bulk fingertip.

Srinivasan proposed a model composed of an elastic membrane filled with an incompressible fluid. The so-called "waterbed" model predicts with a relatively good precision the indentation of the fingerpad with a thin line [149]. These models are also successful at predicting the growth of the area of contact when indenting with a flat surface [137]. The two materials in the model are emulating the role of the skin (the membrane) and the subcutaneous tissues (the fluid). Replacing the membrane by finite-element thin shells allow to accommodate more realistic geometries by still keeping a reasonable computational time [151].

Finite element models have been developed to capture the complex mechanical assembly that is the fingertip and try to unravel the mechanism of tactual perception. The preceding “waterbed” models by their constitution fail to describe the strain inside the tissues and cannot predict the firing of the mechanoreceptive afferents. Moreover, each layer of the skin can be modeled with a accurate geometry. The refine geometry makes possible the investigation of mechanical effects of papilla ridges for instance [93]. Two and three dimensional models have lead to thinks that SA I respond to the strain energy density [29, 146]. These model give a good incentive of the relationship between anatomy and neurology, but the risk of numerical error due to the non-homogeneity of the tissues can be critical for the quality of the results. Dynamic parameters of the skin and subcutaneous tissue can also be modeled and used to predict the viscoelastic behavior of the skin to various dynamic stimulations [180].

2.2.3 Friction Properties on Rough and Smooth Surfaces

Many phenomena are salient to feeling a surface by stroking it with the fingertip. Some of them are related to the viscoelastic behavior, but most of the observations are also based on the unique frictional properties of the finger and skin.

2.2.3.1 Basic Notions of Contact and Tribology

Friction is the reaction force to a motion caused by the relative motion of two surface sliding or rolling on each other. The science behind friction is called tribology, and studies the conditions for various phenomena to arise during relative motion of two surfaces in contact. Two types of friction are often described, adherence (stick) and sliding friction (slip). The former occurs when the contact is not broken and bonds tie both surfaces together. When the tangential force reaches a critical value the bonds break and objects start sliding relative to one another. A force opposite to the motion is still present, but often decreased compared to the one needed to break adherence.

The friction force F_t is proportional to the real area of contact A_r [16]. The latter can be expressed as:

$$F_t = \tau A_r \quad (2.3)$$

with τ the interfacial adhesive stress, which can depend on various parameters like the presence of a fluid between the contacting bodies or chemical properties of both materials [128]. The roughness of both surfaces is also a key factor in the resulting frictional force because it reduces the surface of the real contact area. In the contact region, higher peaks on both sides are touching and the friction force is related to the real contact area of these peaks. The consequence is that the real area of contact is smaller than the apparent area. In the case of rigid materials, the real area

of contact is found by considering the plasticity of the peaks that are compressed $A_r = F_n/\sigma$ where F_n is the normal force applied between both object and σ is the yield stress limit. Amontons's law states that the friction of solid is linear in the coefficient of friction $\mu = F_t/F_n = \tau/\sigma$ and does not depend on the area of contact. This is demonstrated by combining the previous expression with (2.3).

Skin and rubber have similar behavior, sharing a low elastic modulus and a high internal dissipation. During sliding contact with a rigid surface, both behave in a similar fashions [1] and the study of elastic material provides much information about the friction of the skin. In contrast to rigid surfaces, rubber contact does not follow Amontons's law but instead it seems that Van Der Waal's forces on the molecular chains of the rubber are dominant [5]. It follows that the adhesive shear stress has a much higher value but also that the real contact area is close to the apparent value. Therefore for spherical contact, Hertz's theory links the apparent area A_a to the normal force with

$$A_a = \pi \left(\frac{3RF_n}{4E^*} \right)^{\frac{2}{3}} \quad (2.4)$$

with $E^* = \frac{E}{1-\nu^2} = \frac{4}{3}E$ and E is the Young modulus of the soft material, ν is the Poisson coefficient, often taken equal to 0.5 for rubber and skin. R is the radius of curvature of the fingertip providing that the counterbody is flat. This leads to a relationship between the normal and the friction force:

$$F_t = \tau \pi \left(\frac{9RF_n}{16E} \right)^{\frac{2}{3}}. \quad (2.5)$$

The relationship between both forces is not linear by nature even if the materials are taken to be linear. As a more general case, consider that $F_t \propto F_n^{\frac{2}{m}}$ with $2 < m < 3$. For $m = 2$ the contact is based on plasticity, whereas $m = 3$ describes a contact based only on elasticity. Also, considering the roughness of the surface as a self-affine fractal can lead to more complex models that describe the friction behavior with a better accuracy [129].

The adhesive shear stress is correlated with the molecular bond that ties both surfaces. As a consequence, its value depends of the speed of the relative motion. When there is no sliding, and the contact is static, this value is higher than when both surfaces are moving relatively. This can be explained by the fact that the bonds slowly form during static contact and strengthen the adherence. During sliding, the bonds are broken and cannot reform, leading to weaker adhesion. This theory also explains the increase in static friction force with increasing rest time.

2.2.3.2 Static Friction

Grasping and manipulation processes regulate the amount of normal force to avoid slippage, therefore keeping the tangential force below the maximum static friction force [64, 179]. Primates fingertips contact behavior is well explained by Hertz's contact law that is expressed (2.5) [174]. The authors of this study validate the model

with measurements of the real area of contact and deduce that fingerprints do not likely increase friction, as they reduce the real area. In fact, the real area of contact is about 66 % of the apparent area, mostly due to the void that creates ridges.

The adhesive shear stress τ follows a linear relationship with the normal pressure p as follows:

$$\tau = \tau_0 + \alpha p \quad (2.6)$$

where τ_0 and α are coefficients [18]. In the case of glass and polypropylene on skin $\tau_0 = 4.8$ and 6.1 kPa and $\alpha = 0.8$ and 2.0 respectively [1].

The discrepancy between the two materials is explained by the surface free energy. Porous glass is hydrophilic and has low friction whereas polypropylene is hydrophobic and exhibits large friction forces. The behavior is explained by looking at moisture behavior. In the case of hydrophobic materials, water does not have any place to flow and therefore surface tension is amplified [124]. Moreover, moisture softens the *stratum corneum* and therefore the skin is more inclined to fill the contact thus increasing the friction. Production of sweat is believed to be modulated by the body to increase the friction and therefore reduce the require grip force (normal force) [3]. The friction coefficient follows an inverted U-shape curve with the moisture level, being relatively low for dry and wet skin but increases when the skin is damp [4, 161].

Small scale surface roughness ($R_a < 100 \mu\text{m}$)⁴ has an impact on the friction force when stroking the skin against hard material such as metal and plastics [50]. It has been observed that friction decreases with increasing roughness. Similar observations have been made with paper grade [140] and for fabrics [33]. These results agree with the classic tribology theory which states that a smoother surface induces more contact points therefore more friction. For rougher surfaces ($R_a > 100 \mu\text{m}$) however, the friction tends to increase with roughness, but after a certain value the friction force reaches a plateau independently of the surface material [159]. The effect is caused by the skin, which conforms with the surface. The peaks and valleys are separated with a specific spatial period and lock onto the fingerprint ridges. At the beginning of sliding, the skin has to deform to overcome the peaks, increasing the force needed to break contact. Moreover, these protuberances also adhere with the skin, increasing at some point the area of contact [160].

2.2.3.3 Incipient Slip

The transition between stick and sliding states of a fingertip about to slip is a abrupt but not instantaneous event, where the contact is rapidly breaks from the outer ring of the contact toward the center. This event, called incipient slip, comes from the local equilibrium between the normal and the shear interfacial pressure. Hertz contact predicts a quadratic distribution of the normal pressure with maximum pressure

⁴ R_a measurement corresponds to the average of the absolute value of the height of the asperities on the surface.

at the center and zero pressure on the outer ring. Shear stress, however, follows a hyperbolic distribution. Therefore with increasing tangential force, the shear stress will locally overcome the static friction, and the outer region will start to slide [66].

This behavior has been predicted by classical mechanics in the case of rigid solids and has also been observed in the case of the incipient slip of a finger [4, 152]. However the transition does not behave exactly like the classic Midlin–Cattaneo contact theory. This is probably because this model does not consider differences of friction coefficient between the stick and the slip state. If this difference is taken into account, it seems that the end of the transition is characterized by a minimum adhesion area above which the tangential force cannot increase [158].

2.2.3.4 Sliding Friction

Sliding friction occurs when incipient slip ends and all the contact area is in the slip state. At this stage, the finger and the object are moving tangentially relative to each another. In this state of contact, moisture is also a significant factor. On smooth non-porous surfaces, the sweat will accumulate in between the ridges leading to a increase in friction over time. The occlusion of the sweat glands is avoided with porous media, and results to a lower friction force [124]. Velocity, however, does not seem to have a direct or systematic effect on the value of the coefficient of friction.

Stroking a soft or a hard material on non-smooth surface generates vibrations that radiate, in part, as sound. For instance, noise generated by a rigid blade sliding over a rough surface exhibits a sound pressure that is proportional to the roughness estimated, raised to the power 8 to 18. The value of the exponent depends on the inclination of the blade relative to the surface [117]. Such a simple relationship cannot be drawn for finger-surface interaction, because of the complexity of the mechanism at play [2].

The low tangential stiffness of the fingertip makes it prone to stick-slip oscillations. These oscillations appear when an elastic force pulls a slider. If the static and dynamic frictions are not equal, the motion can oscillate between a stick and a slip state. This effect is often present with glass and other smooth non-porous material which exhibit a high friction with the finger [1].

2.2.4 Implication for the Perception with the Bare Finger

Touch is particularly tuned to sense the mechanical phenomena when finger is in static or dynamic contact with various shapes and surfaces.

2.2.4.1 Mechanical Illusions

Similarly to the visual system, the central nervous system does not acquire the complete strain tensors field that results to the contact, but makes simplifications. These

simplifications are based on the fact that mechanoreceptors are sensitive to strain, and also that different directions of the strain at the surface can lead to the same pattern. This information loss creates mechanical tactile illusions.

For instance, if shear stress applied in a band at the center of the fingertip while the outer stays stationary, it is felt as a bump. Finite element analysis reveals that normal and tangential loads produce similar strain patterns at the presumed location of the mechanoreceptor. Since a bump is more common than a lateral stress field, the brain makes sense of the strain pattern by feeling a bump [112]. Similarly, distributed shear stress on the surface well approximates the strain distribution that produces a wave on the surface, at the location of the mechanoreceptors [72, 173].

Viscoelasticity of the tissue also have effects on tactile perception. Moy et al. showed that the relaxation of force during incremental displacement can bias the detection of edges and texture [111]. At last, during sliding of the finger, adding lubricant, decreases the friction, and therefore biases the estimation of roughness [142].

2.2.4.2 Effect of the Fingerprints

There is still much debate about the effect of the fingerprint ridges on tactual perception. It is believed that the papilla ridges, mirrors of the fingerprint ridges, act as levers to magnify the stress [22, 93]. Friction shears the ridges and therefore compresses one of the Meissner corpuscles and stretches the second. Moreover, the presence of ridges concentrates the strain locally and enhances the spatial sensitivity by limiting the cross talk of mechanical stimulus [40].

Another hypothesis looks at the regularity of the contact with the glabrous skin. In fact, the glabrous skin, and especially that found in the fingertip, is subject to mechanical loading for long periods. Ridges could act as a compliant mechanism that avoids damage and strengthens the skin [174]. This strengthening limits the creation of blisters and sores. The finding that the skin is more elastic along the ridges than across them supports the hypothesis that the skin behaves like a deforming bellow [172].

Recently, there has been a debate about the importance of fingerprints in texture perception. Scheibert et al. [135] observed, by means of an artificial finger, that ridges on the surface enhance vibratory signals during perception of fine texture by exciting the frequency where PC afferents are the most sensible. However, this hypothesis was challenged by other researchers, as human fingertips are more complex than simple linear elastic materials [27], and because the presence of fingerprints does not affect signal processing when using finite element analysis [93].

To conclude this overview of the mechanical phenomena that are involved in finger-surface interaction during tactile exploration, it could be observed that the finger is a complex mechanical assembly that adapts to a large variety of shapes and regulates its friction by sweating to optimize grip. Part of the coarse elements of a surface are perceived by the strain field induce by the skin on the shape. The other part of the information is based on the friction noise that is generated during sliding

of the finger. Friction noise is composed of vibrations that propagate in the tissues. Fine texture is inferred from these vibrations, and the spatial distribution of strain is less important. Figure 2.1 summarize the main mechanical events that occurs during sliding of a fingertip on a textured surface.

2.3 Reproduction of Impact and Slip

This section describes a number of devices devoted to the reproduction of tactile sensations. Such devices were motivated by research in diverse areas such as tele-operation, robotic sensing, haptic feedback in virtual reality, and consumer products. The focus is put on those technologies that are able to capture or reproduce sensations of roughness, impact and slip. Interfaces based on pin matrices intended to deform or stretch the skin or surface displays that move a surface under the skin to induce shape sensation will not be discussed in this dissertation. The reader can consult other extensive surveys for additional information on these approaches [8, 122].

2.3.1 *Signal Acquisition*

Researchers have attempted to capture the complexity of the mechanical interactions arising during the exploration of surfaces, either with a probe or with a bare finger. Some studies have been devoted to recording these interactions for haptic simulation or texture perception.

2.3.1.1 Haptic Interaction Recording

In order to record haptic interaction, many projects propose to acquire the high frequency acceleration that is transmitted to the tip of a probe during exploration. A probe sliding on a rough surface is solicited by surface stresses that change through time as the probe moves. The variation of surface stresses induces mechanical vibrations in the probe that can be picked up by accelerometers. With this simple method, roughness can be sensed, recorded, and modeled [83, 118, 119].

In the case of bare finger exploration, sensing interaction forces or skin displacements is more challenging. Ideally the interaction should be measured at the interface between the finger and the surface, but the addition of any type of sensor would necessarily disturb the interaction. It is also possible to measure the displacement of tissues in the finger, for instance by means of a Hall-effect sensor [9], acceleration of the nail [74, 100] or the noise radiated by the finger [155]. These direct measurement techniques employ sensors that are attached to the skin with the following shortcomings. These sensors have a finite mass which may not be negligible compared the impedance of the tissue to which they are attached, perturbing the measurement. But the hardest obstacle is to establish a reliable reconstruction of the skin vibration from distal measurements.

2.3.1.2 Biomimetic Robotics Fingers

Artificial hand research has been focusing on grasping and manipulation. In this context, the tactile sensors, if any, that they include in their design are mostly intended to detect contact and slip. Many are based on an array of sensors that pick up spatially distributed, low frequency interaction in the expectation to detect the shape of the touched object. They are often not well suited for rapid interaction and are sensitive to rapid mechanical transient signals. For recent reviews of these distributed sensors and their fabrication techniques please consult [28, 186].

However, some of the sensors are based on the observation of our sensory system. For instance, Howe et Cutkosky proposed a piezoelectric sensor that reacts to the rate of change of the strain inside a rubber band. This approach mimic the role of Pacinian and authors showed that they could detect slippage and even texture [56, 57]. Robots adjust their grip force accordingly to the captured signal of incipient slip. As for humans, they use the relative tangential motion for the artificial fingers to measure and classify natural textures from the friction-generated vibration [73]. They noted that measuring acceleration rather than displacement is easier for high frequency measurements, as the sensitivity of accelerometer to displacement amplitude evolves with the square of the frequency. Reciprocally, for low frequency and static measurement, displacement gives more signal than acceleration. In the spirit of biomimetism, some artificial fingers are designed to sense the distribution of stick and slip region of the contact and use this information to estimate the ratio of normal and friction force [94, 177]. Fine control and manipulation is achieved by tactually sensing the contact state with the hand-held object.

2.3.2 Reproduction by Force Feedback

To render tactile and kinesthetic sensations, force feedback devices are often used. These devices amount to robotic mechanisms that apply forces relatively to the mechanical ground in response to the displacement of the finger or the hand.

The reproduction of tactual texture with force feedback has been initiated by Minsky during the development of the *Sandpaper* system [105]. They used a two degree-of-freedom (DOF) joystick to synthesize textures. The lateral forces were modulated as a function of the position and of the gradient of the virtual height field. This method produced a sensation on 2D plane that could be associated with roughness [104].

Other algorithms were proposed to extend the rendering of roughness to 3DOF. They used either a oscillating force that is normal, tangential or in both directions to the virtual non-textured surface. Normal forces approaches tend to make the textures feel ‘frictionless’. Texture algorithms themselves can lead to unwanted artifacts and oscillations [21].

The manipulandum and its control is also a critical element for the reproduction with high fidelity. Champion and Hayward used Nyquist and Courant–Friedrichs–Lewy conditions to draw the fundamental limits in terms of force, position and

temporal resolution for correct reproduction [20]. For fine texture reproduction, the resolution of encoder should be as low as $1\text{ }\mu\text{m}$ and the force should be modulated by milli-newtons increments to match human perception thresholds. They also explored the effect of the bandwidth of force feedback and concluded that a device capable of stimulating the finger from DC to 700 Hz with guaranteed stability was difficult to achieve. Commercially available haptic devices, such as the Phantom, are limited by their first structural modes, in this case at 30 Hz.

To overcome the bandwidth limitation several approaches are possible. Transient and rapid mechanical events can be reproduced by vibrotactile shakers mounted on the thimble of force feedback devices [58]. Another approach is to couple two motors of different sizes. The small motor is fast but does not deliver large forces whereas the larger motor produces more torque at the expense of a larger inertia [103]. Another solution is to compensate the narrow bandwidth of a haptic display with an inverse filter. The inverse filter however, should depend on the configuration of the device, which makes the implementation complex [79].

Ordinary force-feedback devices in general suffer from the complexities of their mechanical properties and are prone to introduce instabilities and artifacts.

2.3.3 *Controlled Friction Displays Approaches*

Grounded, electric powered, force-feedback devices are not the only approach to rendering textures. An alternative approach consists of modulating the friction between a surface and the fingertip. This family of devices is increasingly gaining attention because of their compatibility with touchscreen interfaces and the simplicity of their open-loop control.

It is known that surface acoustic waves propagating in rigid substrate can reduce the coefficient of friction between the substrate and an object. Such effect was put to practice by placing an aluminum foil between the fingertip and the surface, eliciting a sensation of reduced stickiness (static reduction) and even roughness (alternative forces) [153]. Electrostatic forces can also be used to change the frictional forces by alternatively attracting and repulsing, regardless of the direction of motion [181].

Electrostatic attraction can also be achieved directly on the fingertip, eliminating the need for an interposed slider. The range of force is greatly reduced and low frequencies cannot be felt. However, if a alternative current of frequency greater than 100 Hz is applied to the electrodes, a vibrotactile sensation is induced when the finger moves [156]. Recently, this technology have been implemented by TeslaTouch [6] and Senseg [97] with the goal to be deployed in multi-touch devices.

Bare finger friction can also be modulated by the squeeze-film effect that exploits the thermodynamic non-linearity of gases. When exciting a plate with normal ultrasonic vibrations, a film of air is pumped under the finger, reducing the friction with the plate. Air pumping was first applied to tactile rendering by Watanabe and Fukui [175]. Two groups, Biet et al. [12] and Windfield et al. [178], later presented devices that uses this phenomenon almost simultaneously. The first group used a standing

wave in a beryllium-copper plate to pump the air below the finger and the other used the first bending mode of a disc piezoelectric transducer to achieve ultrasonic levitation. Improvements have been made such as the use of multiple bending normal mode of a plate to extend applicability to large displays [99].

2.3.4 Vibration Based Displays

Vibrotactile devices do not produce low-frequency forces like force-feedback devices but rather focus on the fact that human perceptual system is most sensitive to high-frequency signals. Exciting the skin with vibrations is an efficient way to elicit tactile sensations.

2.3.4.1 Eccentric Mass Motors

The most common stimulators are the ‘rumble motors’ that are found in almost all cellphones and game controller. Their low price and high efficiency make them the technology of choice for alarm-type tactile signals. The stimulator is a DC motor with an eccentric mass attached to the shaft. Activation creates rotating radial forces due to the eccentricity. Despite its simplicity and efficiency, this technology is ill-suited for generating rich sensations since signal amplitude and the frequency are inherently coupled from the principle of operation. They also suffer from poor temporal resolution.

2.3.4.2 Electromagnetic Shakers and Recoil Motors

Richer vibrotactile sensations are made possible by the inertial motor based on voice-coil transducers or on piezoelectric actuators. They can be applied to vibrate the screen or the enclosure of a device to produce tactile sensations [39]. It can also or be used to directly stimulate the skin [109, 184]. Voice-coil actuators use Laplace forces to move a magnet suspended in the housing by a membrane. The magnet serves as the inertial slug and moves over a single degree of freedom. The moving slug, driven above the resonant frequency, creates a force that pushes back by conservation of momentum on the housing and therefore on the skin. These recoil motors can reproduce acceleration over a large bandwidth (typically 50 Hz to several kHz) being limited in the low frequency by the suspension elasticity, maximum displacement, and the mass of the slug. In the high frequencies, the structural modes determine the limit of the response. It is advantageous to design-in a low coefficient of quality to damp the resonance and extend the flat bandwidth.

Recoil motors enable fine control over of vibrotactile signal without the need of a ground reference. They have been used in many demonstrations. Yao et al. described a stick equipped with such voice-coil motor to simulate a virtual rolling ball

[183]. Textural sensations can also be created with pen-based interfaces by inducing vibrations in the stylus [133]. Larger motors can be used to stimulate the foot, and give the sensation of walking on virtual floor such as sand or ice [171].

2.3.4.3 Linear Resonant Actuators

Some application use linear-resonant actuators (LRA) to create a tactile sensation by amplitude modulation of a vibration at a resonant frequency. LRA have the same basic construction a recoil motors, but their coefficient of quality is much higher and they are usually less powerful. As a consequence only the resonant frequency can be felt [34]. Complex signals are usually generated by amplitude modulation. To increase efficiency, the inertial slug can intentionally be designed to impact the enclosure, creating a strong, but hard-to-control, acceleration pattern [182].

2.3.4.4 Piezoelectric Devices

Many researchers attempted to replace electromagnetic drives by other actuation means such as shape memory alloys, pneumatic, electroactive polymers and so on. These novel actuation approaches rarely reach sufficient maturity to be attractive for the consumer electronic market, due to various limitations arising from high drive voltages, manufacturing difficulties or lack of reliability. Piezoelectric transducers on the other hand can be exceedingly practical.

Piezoelectricity is the property of crystals to displace charges in a material when it is strained. Conversely, electrostatic fields applied across the material induce mechanical deformations. Owing to the large number of application of these transducers, ceramics have been developed to enhance the achievable strains. A common material is the lead-zirconate-titanate ceramic, also named PZT, which can deform to a maximum strain of about 0.1 %.

Stacking, and other mechanical arrangements of thin PZT plates, are often necessary to achieve a workable stroke displacement for a given actuator size. Piezoelectric actuators are often used in the form of bending bimorphs, which are composed of two plates bonded together and actuated in opposition. The compression of one side and the stretching of the other causes the blade to bend, achieving displacements that can reach several millimeters under reasonable voltages.

These piezoelectric bimorphs are, for instance, responsible of the motion of the pins in Braille cells [162]. They are also used to move an inertial slug inside an enclosure, or directly vibrate the screen of a portable device[132]. Their natural stiffness and low damping makes them efficient when used at resonance.

Similarly to electromagnetic LRA's, tactile signals can be generated by amplitude-modulation. Maeno et al. applied this idea to reproduce virtual textures by using an ultrasonic motor modulated with the amplitude of the measurement made by a sliding probe [95].

2.3.5 *Simulated Material and Textures*

Actuators are driven accordingly to the user's input. In force-feedback devices, a force is specified in response to a position input (the impedance approach). Another approach is to regulate the velocity of a handle according to an input force (the admittance approach). This section reviews the various algorithms that synthesize realistic tactile sensation accordingly to a virtual representation of the world. Most algorithms are based on the assumption that a contact can be approximated by the behavior of a single point impacting or sliding in the virtual world.

2.3.5.1 **Impact**

Impact transients and high frequency oscillations add realism to haptic simulations in virtual environments. Okamura et al. [116] proposed a methodology to acquire oscillations generated by the impact with real materials. The measured response was modeled by decaying sinusoids which coefficients that best fit the transient. Hard material exhibit higher frequency and lower decay rate, whereas soft material like rubber damp the collision. During the simulation, transients are replayed by adding the decaying sinusoid with amplitude proportional to the impact velocity to the amplitude of the force signal. Instead of using only one damped sinusoid, a sum of decaying sinusoid can be used to model the modal response of more complex object to an impact [163]. The impact location can also affect the vibration signature. For instance, a beam produces modal vibrations that depend on the location of an impact. Reproducing this effects is sufficient to give to the user the sensation of the impact location [145].

2.3.5.2 **Roughness**

Virtual textures synthesis tools rely on physical properties of real textures. Siira and Pai noticed that many textured surfaces were characterized by a height Gaussian distribution. As a result, they proposed a stochastic model to synthesize textures by addition of a random component to the rendering of a smooth surface. They took advantage of the fact that normal distribution is independent of resampling and that the norm and standard deviation did not depend on velocity. This observation led to a simplified computation able to generate white surface noise at every increment of time. The simplicity of the rendering in the temporal domain has the disadvantage that the spatial consistency is not maintained. As a result, the same point in space could be rendered with different values [139].

The stochastic model was extended to render other features of textures. Bump and deterministic geometries can be modeled by their Fourier decomposition and the stochastic behavior described by a sum of Gaussian distributions. Other random processes such as band-limited noise or banks of filtered noise can be used to replace the Gaussian white noise distribution [38]. A texture model described in the spatial

domain was then interpolated in the temporal domain for rendering. Perceptually, it was found that the roughness sensations were correlated with the standard deviation of the Gaussian distribution.

The idea of space-based description has been used by van den Doen et al. [164] to render the sounds produced by stoking a stick on a surface at audio rates. To reproduce the recording, they used a “phonograph needle” model. Samples were recorded at constant speed, v_{ref} , and replayed at a rate of v/v_{ref} by interpolating the missing samples. Moreover, the audio volume was scaled by the square root of the power dissipated by friction. If friction is assumed to follow Amonton’s law of friction, then the acoustic signal is $a(t) \propto \sqrt{\mu|F_n v|}$ where μ is the coefficient of dynamic friction, F_n the normal force, and v the velocity.

Surface topology can also be described by fractal noise. Fractals are irregular self-similar structures often found in nature processes [98]. Costa et al. [26] computed the height profile of a textured surface by synthesizing the signal as a Fourier series which coefficients generated by $1/f^\beta$ power spectral noise density. Experiment indicated that the roughness estimates were strongly correlated with the root-mean-square of the height profile. Different fractal dimensions evoked different textures.

2.3.5.3 Friction Related Events

Other phenomena, such as stick-slip oscillations, have been virtually rendered. Stick-slip oscillations occur when the friction force is higher during the stuck state than during the slip state and when there is a forcing term. When these conditions are met, a system can oscillates between the stuck state and the slip state according to the mean velocity. Konyo et al. proposed to trigger a 250 Hz decaying sinusoids produced by a piezoelectric transducer at the transitions to provide a simulated feeling of incipient slip under the bare finger [77].

2.4 Conclusion

Texture is an important attribute of the objects; it has therefore received a commensurate amount of attention in the literature. The amount of realism of virtual environment depends greatly on the fidelity of the visual, audio, and haptic texture models. Much work has been dedicated to the understanding of perception of texture through direct contact with a bare finger. The consensus is that the sensation of roughness plays a central role in the perception of textures and that roughness sensations are mediated by rapid mechanical events rather than spatially coded information.

To date, research regarding the encoding of tactual roughness encoding and its artificial reproduction has been mainly focused on the rigid-probe model. This focus is easy to explain since recording the vibrations of a probe stroking a surface

only requires an accelerometer and reproduction can be accomplished with force-feedback devices and/or vibrotactile transducers. In the case of a bare finger the contact condition are fundamentally different from that of a rigid probe. The analysis and the modeling of the mechanics of interaction no longer can be reduced to the movements of a rigid body. It is necessary to account for the mechanical properties of a fingertip and for skin tribology to gain an appreciation of the complexity of the interaction.

Research in biomechanics and skin tribology was to date mostly motivated by issues in motor control (grip), as well as by health and cosmetics research. As a result, the complex interactions arising during sliding on a surface have been by-and-large ignored. For instance, most studies assume quasi-static conditions or very low frequencies. Psychophysics of touch, in contrast, reveals that tactile perception operates within a range that reaches DC to 700 Hz. Moreover, very little work has been devoted to the characterization of vibrations generated when stroking a finger on surfaces.

If this challenges were solved it would be possible to transfer the knowledge of physical interactions to the rendering more realistic artificial sensations. The enhancement of the rendering techniques could be the beginning of high fidelity tactile devices and can possibly spread to several domains of applications. Transducer design would also be improved and simplified by the knowledge of the mechanics of touch.

References

1. Adams MJ, Briscoe BJ, Johnson SA (2007) Friction and lubrication of human skin. *Tribol Lett* 26(3):239–253
2. Akay A (2002) Acoustics of friction. *J Acoust Soc Am* 111:1525
3. André T, Lefèvre P, Thonnard JL (2010) Fingertip moisture is optimally modulated during object manipulation. *J Neurophysiol* 103(1):402–408
4. André T, Lévesque V, Hayward V, Lefèvre P, Thonnard JL (2011) Effect of skin hydration on the dynamics of fingertip gripping contact. *J R Soc Interface*
5. Barquins M (1993) Friction and wear of rubber-like materials. *Wear* 160(1):1–11
6. Bau O, Poupyrev I, Israr A, Harrison C (2010) TeslaTouch: electrovibration for touch surfaces. In: *Proceedings of the 23rd annual ACM symposium on user interface software and technology*, ACM, New York, pp 283–292
7. Bell J, Bolanowski S, Holmes MH (1994) The structure and function of pacinian corpuscles: a review. *Prog Neurobiol* 42(1):79–128
8. Benali-Khoudja M, Hafez M, Alexandre JM, Kheddar A (2004) Tactile interfaces: a state-of-the-art survey. In: *Int symposium on robotics*
9. Bensmaïa SJ, Hollins M (2003) The vibrations of texture. *Somatosens Motor Res* 20(1):33–43
10. Bensmaïa SJ, Hollins M (2000) Complex tactile waveform discrimination. *J Acoust Soc Am* 108(3):1236–1245
11. Bergmann-Tiest WM, Kappers AML (2006) Analysis of haptic perception of materials by multidimensional scaling and physical measurements of roughness and compressibility. *Acta Psychol* 121(1):1–20
12. Biet M, Giraud F, Lemaire-Semail B (2007) Squeeze film effect for the design of an ultrasonic tactile plate. *IEEE Trans Ultrason Ferroelectr Freq Control* 54(12):2678–2688

13. Birznieks I, Macefield VG, Westling G, Johansson RS (2009) Slowly adapting mechanoreceptors in the borders of the human fingernail encode fingertip forces. *J Neurosci* 29(29):9370
14. Blake DT, Johnson KO, Hsiao SS (1997) Monkey cutaneous SA I and Ra responses to raised and depressed scanned patterns: effects of width, height, orientation, and a raised surround. *J Neurophysiol* 78(5):2503
15. Bolanowski SJ, Gescheider GA, Verrillo RT, Checkosky CM (1988) Four channels mediate the mechanical aspects of touch. *J Acoust Soc Am* 84(5):1680–1684
16. Bowden FP, Tabor D (1939) The area of contact between stationary and between moving surfaces. *Proc R Soc Lond Ser A, Math Phys Sci*, 391–413
17. Brisben AJ, Hsiao SS, Johnson KO (1999) Detection of vibration transmitted through an object grasped in the hand. *J Neurophysiol* 81(4):1548
18. Briscoe BJ, Tabor D (1975) The effect of pressure on the frictional properties of polymers. *Wear* 34(1):29–38
19. Cadoret G, Smith AM (1996) Friction, not texture, dictates grip forces used during object manipulation. *J Neurophysiol* 75(5):1963
20. Campion G, Hayward V (2005) Fundamental limits in the rendering of virtual haptic textures. In: *Proceedings of the first joint eurohaptics conference and symposium on haptic interfaces for virtual environment and teleoperator systems*, pp 263–270
21. Campion G, Hayward V (2008) On the synthesis of haptic textures. *IEEE Trans Robot* 24(3):527–536
22. Cauna N (1954) Nature and functions of the papillary ridges of the digital skin. *Anat Rec* 119(4):449–468
23. Chambers MR, Andres KH, Duering M, Iggo A (1972) The structure and function of the slowly adapting type II mechanoreceptor in hairy skin. *Exp Physiol* 57(4):417
24. Cohen JC, Makous JC, Bolanowski SJ (1999) Under which conditions do the skin and probe decouple during sinusoidal vibrations? *Exp Brain Res* 129:211–217
25. Connor CE, Johnson KO (1992) Neural coding of tactile texture: comparison of spatial and temporal mechanisms for roughness perception. *J Neurosci* 12(9):3414
26. Costa MA, Cutkosky MR (2000) Roughness perception of haptically displayed fractal surfaces. In: *Proceedings of the ASME dynamic systems and control division*, vol 69, pp 1073–1079
27. Dahiya RS, Gori M (2010) Probing with and into fingerprints. *J Neurophysiol* 104(1):1
28. Dahiya RS, Metta G, Valle M, Sandini G (2010) Tactile sensing—from humans to humanoid. *IEEE Trans Robot* 26(1):1–20
29. Dandekar K, Raju BI, Srinivasan MA (2003) 3-d finite-element models of human and monkey fingertips to investigate the mechanics of tactile sense. *J Biomech Eng* 125:682
30. Delhaye B, Hayward V, Lefevre P, Thonnard JL (2010) Textural vibrations in the forearm during tactile exploration. Poster 782.11. In: *Annual meeting of the society for neuroscience*
31. Delmas P, Hao J, Rodat-Despoix L (2011) Molecular mechanisms of mechanotransduction in mammalian sensory neurons. *Nat Rev Neurosci* 12(3):139–153
32. Dépeault A, Meftah EM, Chapman CE (2008) Tactile speed scaling: contributions of time and space. *J Neurophysiol* 99(3):1422
33. Derler S, Schrader U, Gerhardt LC (2007) Tribology of human skin and mechanical skin equivalents in contact with textiles. *Wear* 263(7–12):1112–1116
34. Do Kweon S, Park IIO, Son YH, Choi J, Oh HY (2008) Linear vibration motor using resonance frequency. Google patents. US patent 7,358,633
35. Ekman G, Hosman J, Lindstrom B (1965) Roughness, smoothness, and preference: a study of quantitative relations in individual subjects. *J Exp Psychol* 70(1):18
36. Essick GK, Franzen O, Whitsel BL (1988) Discrimination and scaling of velocity of stimulus motion across the skin. *Somatosens Motor Res* 6(1):21–40
37. Fearing RS, Hollerbach JM (1985) Basic solid mechanics for tactile sensing. *Int J Robot Res* 4(3):40

38. Fritz JP, Barner KE (1996) Stochastic models for haptic texture. In: Proceedings of SPIE's international symposium on intelligent systems and advanced manufacturing—telem manipulator and telepresence technologies III, pp 34–44
39. Fukumoto M, Sugimura T (2001) Active click: tactile feedback for touch panels. In: CHI'01 extended abstracts on human factors in computing systems, ACM, New York, pp 121–122
40. Gerling GJ, Thomas GW (2005) The effect of fingertip microstructures on tactile edge perception. In: Proceedings of the first joint eurohaptics conference and symposium on haptic interfaces for virtual environment and teleoperator systems, IEEE Computer Society, Los Alamitos, pp 63–72
41. Gescheider GA, Bolanowski Jr SJ, Verrillo RT, Arpajian DJ, Ryan TF (1990) Vibrotactile intensity discrimination measured by three methods. *J Acoust Soc Am* 87:330
42. Gescheider GA, Bolanowski SJ, Greenfield TC, Brunette KE (2005) Perception of the tactile texture of raised-dot patterns: a multidimensional analysis. *Somatosens Motor Res* 22(3):127–140
43. Gibson JJ (1962) Observations on active touch. *Psychol Rev* 69(6):477
44. von Gierke HE, Oestreicher HL, Franke EK, Parrack HO, von Wittern WW (1952) Physics of vibrations in living tissues. *J Appl Physiol* 4(12):886
45. Goff GD (1967) Differential discrimination of frequency of cutaneous mechanical vibration. *J Exp Psychol* 74(2):294–299
46. Goodwin AW, Morley JW (1987) Sinusoidal movement of a grating across the monkey's fingerpad: representation of grating and movement features in afferent fiber responses. *J Neurosci* 7(7):2168
47. Goodwin AW, Macefield VG, Bisley JW (1997) Encoding of object curvature by tactile afferents from human fingers. *J Neurophysiol* 78(6):2881
48. Hajian AZ, Howe RD (1997) Identification of the mechanical impedance at the human finger tip. *J Biomech Eng* 119:109
49. Halata Z, Grim M, Bauman KI (2003) Friedrich Sigmund Merkel and his “Merkel cell”, morphology, development, and physiology: review and new results. *Anat Rec, Part A Discov Mol Cell Evol Biol* 271(1):225–239
50. Hendriks C, Franklin S (2010) Influence of surface roughness, material and climate conditions on the friction of human skin. *Tribol Lett* 37:361–373
51. Hollins M, Risner SR (2000) Evidence for the duplex theory of tactile texture perception. *Atten Percept Psychophys* 62(4):695–705
52. Hollins M, Faldowski R, Rao S, Young F (1993) Perceptual dimensions of tactile surface texture: a multidimensional scaling analysis. *Percept Psychophys* 54(6):697–705
53. Hollins M, Bensmaïa SJ, Karlof K, Young F (2000) Individual differences in perceptual space for tactile textures: evidence from multidimensional scaling. *Atten Percept Psychophys* 62:1534–1544
54. Hollins M, Bensmaïa SJ, Washburn S (2001) Vibrotactile adaptation impairs discrimination of fine, but not coarse, textures. *Somatosens Motor Res* 18(4):253–262
55. Hollins M, Bensmaïa SJ, Roy EA (2002) Vibrotaction and texture perception. *Behav Brain Res* 135(1–2):51–56
56. Howe RD, Cutkosky MR (1989) Sensing skin acceleration for slip and texture perception. In: Proceedings of the 1989 IEEE international conference on robotics and automation, pp 145–150
57. Howe RD, Cutkosky MR (1993) Dynamic tactile sensing: perception of fine surface features with stress rate sensing. *IEEE Trans Robot Autom* 9(2):140–151
58. Howe RD, Kontarinis D (1994) High-frequency force information in teleoperated manipulation. *Exp Robot III*:341–352
59. Israr A, Choi S, Tan HZ (2006) Detection threshold and mechanical impedance of the hand in a pen-hold posture. In: 2006 IEEE/RSJ international conference on intelligent robots and systems, IEEE, New York, pp 472–477

60. Israr A, Choi S, Tan HZ (2007) Mechanical impedance of the hand holding a spherical tool at threshold and suprathreshold stimulation levels. In: World haptics 2007, IEEE, New York, pp 56–60
61. Jindrich DL, Zhou Y, Becker T, Dennerlein JT (2003) Non-linear viscoelastic models predict fingertip pulp force-displacement characteristics during voluntary tapping. *J Biomech* 36(4):497–503
62. Johansson RS, LaMotte RH (1983) Tactile detection thresholds for a single asperity on an otherwise smooth surface. *Somatosens Motor Res* 1(1):21–31
63. Johansson RS, Vallbo AB (1979) Tactile sensibility in the human hand: relative and absolute densities of four types of mechanoreceptive units in glabrous skin. *J Physiol* 286(1):283
64. Johansson RS, Westling G (1984) Roles of glabrous skin receptors and sensorimotor memory in automatic control of precision grip when lifting rougher or more slippery objects. *Exp Brain Res* 56(3):550–564
65. Johansson RS, Landström U, Lundström R (1982) Responses of mechanoreceptive afferent units in the glabrous skin of the human hand to sinusoidal skin displacements. *Brain Res* 244(1):17–25
66. Johnson KL (1987) Contact mechanics. Cambridge University Press, Cambridge
67. Johnson KO (2001) The roles and functions of cutaneous mechanoreceptors. *Curr Opin Neurobiol* 11(4):455–461
68. Johnson KO, Hsiao SS (1992) Neural mechanisms of tactual form and texture perception. *Annu Rev Neurosci* 15(1):227–250
69. Johnson KO, Phillips JR (1981) Tactile spatial resolution. I. Two-point discrimination, gap detection, grating resolution, and letter recognition. *J Neurophysiol* 46(6):1177
70. Johnson KO, Yoshioka T, Vega-Bermudez F (2000) Tactile functions of mechanoreceptive afferents innervating the hand. *J Clin Neurophysiol* 17(6):539
71. Katz D (1925) The world of touch. Original work published in Erlbaum, Hillsdale, NJ
72. Kikuuwe R, Sano A, Mochiyama H, Takesue N, Fujimoto H (2005) Enhancing haptic detection of surface undulation. *ACM Trans Appl Percept* 2(1):46–67
73. Kim SH, Engel J, Liu C, Jones DL (2005) Texture classification using a polymer-based mems tactile sensor. *J Micromech Microeng* 15:912
74. Kim YS, Kesavadas T (2006) Material property recognition by active tapping for fingertip digitizing. In: 14th symposium on haptic interfaces for virtual environment and teleoperator systems, IEEE, New York, pp 133–139
75. Klatzky RL, Lederman SJ (1999) Tactile roughness perception with a rigid link interposed between skin and surface. *Percept Psychophys* 61(4):591–607
76. Knibestöl M, Vallbo ÅB (1980) Intensity of sensation related to activity of slowly adapting mechanoreceptive units in the human hand. *J Physiol* 300(1):251
77. Konyo M, Yamada H, Okamoto S, Tadokoro S (2008) Alternative display of friction represented by tactile stimulation without tangential force. In: Haptics: perception, devices and scenarios, pp 619–629
78. Krueger LE (1982) Tactual perception in historical perspective: David Katz's world of touch. In: Schiff W, Foulke E (eds) Tactual perception; a sourcebook. Cambridge University Press, Cambridge, pp 1–55
79. Kuchenbecker KJ, Niemeyer G (2006) Improving telerobotic touch via high-frequency acceleration matching. In: Proceedings of 2006 IEEE international conference on robotics and automation, IEEE, New York, pp 3893–3898
80. Lamb GD (1983) Tactile discrimination of textured surfaces: psychophysical performance measurements in humans. *J Physiol* 338(1):551
81. LaMotte RH, Mountcastle VB (1975) Capacities of humans and monkeys to discriminate vibratory stimuli of different frequency and amplitude: a correlation between neural events and psychological measurements. *J Neurophysiol* 38(3):539
82. LaMotte RH, Srinivasan MA (1991) Surface microgeometry: tactile perception and neural encoding. In: Wenner–Gren international symposium series, pp 49–58

83. Lang J, Andrews S (2011) Measurement-based modeling of contact forces and textures for haptic rendering. *IEEE Trans Vis Comput Graph* 17(3):380–391
84. Lederman SJ, Klatzky RL (1987) Hand movements: a window into haptic object recognition. *Cogn Psychol* 19(3):342–368
85. Lederman SJ, Klatzky RL (1997) Designing haptic interfaces for teleoperational and virtual environments: should spatially distributed forces be displayed to the fingertip. In: *Proc of the ASME dynamic systems and control division, symposium on haptic interfaces, DSC*, vol 59
86. Lederman SJ, Taylor MM (1972) Fingertip force, surface geometry, and the perception of roughness by active touch. *Percept Psychophys* 12(5):401–408
87. Lederman SJ, Loomis JM, Williams DA (1982) The role of vibration in the tactual perception of roughness. *Atten Percept Psychophys* 32(2):109–116
88. Lederman SJ, Klatzky RL, Hamilton CL, Ramsay GI (1999) Perceiving roughness via a rigid probe: psychophysical effects of exploration speed and mode of touch. *Haptics-e* 1(1) (<http://www.haptics-e.org>). doi:10.1.1.42.4553
89. Levesque V, Hayward V (2003) Experimental evidence of lateral skin strain during tactile exploration. In: *Proc Eurohaptics 2003*, pp 261–275
90. Libouton X, Barbier O, Plaghki L, Thonnard JL (2010) Tactile roughness discrimination threshold is unrelated to tactile spatial acuity. *Behav Brain Res* 208:473–478
91. Louw S, Kappers AML, Koenderink JJ (2000) Haptic detection thresholds of Gaussian profiles over the whole range of spatial scales. *Exp Brain Res* 132(3):369–374
92. Lundström RJ (1986) Responses of mechanoreceptive afferent units in the glabrous skin of the human hand to vibration. *Scand J Work, Environ. & Health* 12(4 Spec No):413
93. Maeno T, Kobayashi K, Yamazaki N (1998) Relationship between the structure of human finger tissue and the location of tactile receptors. *JSME Int J Ser C, Dyn Control Robot Des Manuf* 41(1):94–100
94. Maeno T, Hiromitsu S, Kawai T (2000) Control of grasping force by detecting stick/slip distribution at the curved surface of an elastic finger. In: *IEEE international conference on robotics and automation, 2000*, vol 4, IEEE, New York, pp 3895–3900
95. Maeno T, Otokawa K, Konyo M (2006) Tactile display of surface texture by use of amplitude modulation of ultrasonic vibration. In: *Proceedings of the IEEE ultrasonics symposium*, pp 62–65
96. Mahns DA, Perkins NM, Sahai V, Robinson L, Rowe MJ (2005) Vibrotactile frequency discrimination in human hairy skin. *J Neurophysiol* 95(3):1442–1450
97. Makinen V, Linjama J, Gulzar Z (2010) Tactile stimulation apparatus having a composite section comprising a semiconducting material. Google patents. US patent App. 12/900,305
98. Mandelbrot BB (1982) *The fractal geometry of nature*. Freeman, New York
99. Marchuk ND, Colgate JE, Peshkin MA (2010) Friction measurements on a large area tpad. In: *Haptics symposium, 2010, IEEE, New York*, pp 317–320
100. Martinot F, Houzeff A, Biet M, Chaillou C (2006) Mechanical responses of the fingerpad and distal phalanx to friction of a grooved surface: effect of the contact angle. In: *Proceedings of the IEEE conference on virtual reality*, p 99
101. Meenes M, Zigler MJ (1923) An experimental study of the perceptions roughness and smoothness. *Am J Psychol*, 542–549
102. Meftah EM, Belingard L, Chapman CE (2000) Relative effects of the spatial and temporal characteristics of scanned surfaces on human perception of tactile roughness using passive touch. *Exp Brain Res* 132(3):351–361
103. Millet G, Haliyo S, Regnier S, Hayward V (2009) The ultimate haptic device: first step. In: *IEEE world haptics conference 2009*, pp 273–278
104. Minsky M, Lederman SJ (1996) Simulated haptic textures: roughness. In: *Proceedings of the ASME dynamic systems and control division*, vol 58, pp 421–426
105. Minsky M, Ming O, Steele O, Brooks Jr FP, Behensky M (1990) Feeling and seeing: issues in force display. In: *Proceedings of the 1990 symposium on interactive 3D graphics*, ACM, New York, pp 235–241

106. Miyaoka T, Mano T, Ohka M (1999) Mechanisms of fine-surface-texture discrimination in human tactile sensation. *J Acoust Soc Am* 105:2485
107. Monzée J, Lamarre Y, Smith AM (2003) The effects of digital anesthesia on force control using a precision grip. *J Neurophysiol* 89(2):672
108. Morley JW, Goodwin AW, Darian-Smith I (1983) Tactile discrimination of gratings. *Exp Brain Res* 49(2):291–299
109. Mortimer BJ, Zets GA, Cholewiak RW (2007) Vibrotactile transduction and transducers. *J Acoust Soc Am* 121(5 Pt 1):2970
110. Mountcastle VB, LaMotte RH, Carli G (1972) Detection thresholds for stimuli in humans and monkeys: comparison with threshold events in mechanoreceptive afferent nerve fibers innervating the monkey hand. *J Neurophysiol* 35(1):122
111. Moy G, Singh U, Tan E, Fearing RS (2000) Human psychophysics for teletaction system design. *Haptics-e* 1(3):1–20
112. Nakatani M, Sato A, Tachi S, Hayward V (2008) Tactile illusion caused by tangential skin strain and analysis in terms of skin deformation. In: *Haptics: perception, devices and scenarios*, pp 229–237
113. Nakazawa N, Ikeura R, Inooka H (2000) Characteristics of human fingertips in the shearing direction. *Biol Cybern* 82(3):207–214
114. Nefs HT, Kappers AML, Koenderink JJ (2002) Frequency discrimination between and within line gratings by dynamic touch. *Atten Percept Psychophys* 64(6):969–980
115. Nefs HT, Kappers AML, Koenderink JJ (2001) Amplitude and spatial-period discrimination in sinusoidal gratings by dynamic touch. *Perception* 30:1263–1274
116. Okamura AM, Cutkosky MR, Dennerlein JT (2001) Reality-based models for vibration feedback in virtual environments. *IEEE/ASME Trans Mechatron* 6(3):245–252
117. Othman MO, Elkholy AH (1990) Surface-roughness measurement using dry friction noise. *Exp Mech* 30(3):309–312
118. Pai DK, Rizun P (2003) The what: a wireless haptic texture sensor. In: *11th symposium on haptic interfaces for virtual environment and teleoperator systems. HAPTICS 2003*, IEEE, New York, pp 3–9
119. Pai DK, Doel K, James DL, Lang J, Lloyd JE, Richmond JL, Yau SH (2001) Scanning physical interaction behavior of 3d objects. In: *Proceedings of the 28th annual conference on computer graphics and interactive techniques*, pp 87–96
120. Paré M, Elde R, Mazurkiewicz JE, Smith AM, Rice FL (2001) The meissner corpuscle revisited: a multiafferented mechanoreceptor with nociceptor immunochemical properties. *J Neurosci* 21(18):7236
121. Paré M, Behets C, Cornu O (2003) Paucity of presumptive ruffini corpuscles in the index finger pad of humans. *J Comp Neurol* 456(3):260–266
122. Pasquero J (2006) Survey on communication through touch. Technical report TR-CIM-06.04, Center for Intelligent Machines, McGill University
123. Pastor MA, Day BL, Macaluso E, Friston KJ, Frackowiak RSJ (2004) The functional neuroanatomy of temporal discrimination. *J Neurosci* 24(10):2585
124. Pasumarty S, Johnson S, Watson S, Adams MJ (2011) Friction of the human finger pad: Influence of moisture, occlusion and velocity. *Tribol Lett* 44(2):117–137
125. Pataky TC, Latash ML, Zatsiorsky VM (2005) Viscoelastic response of the finger pad to incremental tangential displacements. *J Biomech* 38:1441–1449
126. Pawluk DTV, Howe RD (1999) Dynamic contact of the human fingerpad against a flat surface. *J Biomech Eng* 121:605
127. Pawluk DTV, Howe RD (1999) Dynamic lumped element response of the human fingerpad. *ASME J Biomech Eng* 121:178–184
128. Persson BNJ (2000) *Sliding friction: physical principles and applications*, vol 1. Springer, Berlin
129. Persson BNJ (2001) Theory of Rubber friction and contact mechanics. *J Chem Phys* 115(8):3840–3861

130. Phillips JR, Johnson KO (1981) Tactile spatial resolution. II. Neural representation of bars, edges, and gratings in monkey primary afferents. *J Neurophysiol* 46(6):1192
131. Picard D, Dacremont C, Valentin D, Giboreau A (2003) Perceptual dimensions of tactile textures. *Acta Psychol* 114(2):165–184
132. Poupyrev I, Rekimoto J, Maruyama S (2007) Mobile apparatus having tactile feedback function. Google patents. US patent 7,205,978
133. Romano JM, Yoshioka T, Kuchenbecker KJ (2010) Automatic filter design for synthesis of haptic textures from recorded acceleration data. In: 2010 IEEE international conference on robotics and automation, IEEE, New York, pp 1815–1821
134. Sathian K, Goodwin AW, John KT, Darian-Smith I (1989) Perceived roughness of a grating: correlation with responses of mechanoreceptive afferents innervating the monkey's fingerpad. *J Neurosci* 9(4):1273
135. Scheibert J, Leurent S, Prevost A, Debregeas G (2009) The role of fingerprints in the coding of tactile information probed with a biomimetic sensor. *Science* 323:1503–1506
136. Serina ER, Mote CD, Rempel D (1997) Force response of the fingertip pulp to repeated compression—effects of loading rate, loading angle and anthropometry. *J Biomech* 30(10):1035–1040
137. Serina ER, Mockensturm E, Mote CD, Rempel D (1998) A structural model of the forced compression of the fingertip pulp. *J Biomech* 31(7):639–646
138. Shrewsbury M, Johnson RK (1975) The fascia of the distal phalanx. *J Bone Jt Surg, Am Vol* 57(6):784
139. Siira J, Pai DK (1996) Haptic texturing—a stochastic approach. In: IEEE international conference on robotics and automation, 1996, vol 1, IEEE, New York, pp 557–562
140. Skedung L, Danerlöv K, Olofsson U, Aikala M, Niemi K, Kettle J, Rutland MW (2010) Finger friction measurements on coated and uncoated printing papers. *Tribol Lett* 37(2):389–399
141. Smith AM, Scott SH (1996) Subjective scaling of smooth surface friction. *J Neurophysiol* 75(5):1957
142. Smith AM, Chapman CE, Deslandes M, Langlais JS, Thibodeau MP (2002) Role of friction and tangential force variation in the subjective scaling of tactile roughness. *Exp Brain Res* 144(2):211–223
143. Smith AM, Basile G, Theriault-Groom J, Fortier-Poisson P, Campion G, Hayward V (2010) Roughness of simulated surfaces examined with a haptic tool; effects of spatial period, friction, and resistance amplitude. *Exp Brain Res* 202(1):33–43
144. Soneda T, Nakano K (2010) Investigation of vibrotactile sensation of human fingerpads by observation of contact zones. *Tribol Int* 43(1–2):210–217
145. Sreng J, Lécuyer A, Andriot C (2008) Using vibration patterns to provide impact position information in haptic manipulation of virtual objects. In: *Haptics: perception, devices and scenarios*, pp. 589–598
146. Srinivasan M, Dandekar K (1996) An investigation of the mechanics of tactile sense using two-dimensional models of the primate fingertip. *J Biomech Eng* 118(1):48
147. Srinivasan MA, Whitehouse JM, LaMotte RH (1990) Tactile detection of slip: surface microgeometry and peripheral neural codes. *J Neurophysiol* 63(6):1323
148. Srinivasan M, Gulati RJ, Dandekar K (1992) In vivo compressibility of the human fingertip. *ASME Adv Bioeng* 22:573–576
149. Srinivasan MA (1989) Surface deflection of primate fingertip under line load. *J Biomech* 22(4):343–349
150. Stevens JC, Harris JR (1962) The scaling of subjective roughness and smoothness. *J Exp Psychol* 64:489–494
151. Tada M, Pai DK (2008) Finger shell: predicting finger pad deformation under line loading. In: *Proceedings of the 2008 symposium on haptic interfaces for virtual environment and teleoperator systems*, IEEE Computer Society, Los Alamitos, pp 107–112
152. Tada M, Mochimaru M, Kanade T (2006) How does a fingertip slip?—contact mechanics of a fingertip under tangential loading. In: *EuroHaptics 2006*, pp 415–420

153. Takasaki M, Kotani H, Nara T, Mizuno T (2005) Transparent surface acoustic wave tactile display. In: Proceedings of the IEEE/RSJ international conference on intelligent robots and systems, pp 1115–1120
154. Talbot WH, Darian-Smith I, Kornhuber HH, Mountcastle VB (1968) The sense of flutter-vibration: comparison of the human capacity with response patterns of mechanoreceptive afferents from the monkey hand. *J Neurophysiol* 31(2):301
155. Tanaka Y, Horita Y, Sano A, Fujimoto H (2011) Tactile sensing utilizing human tactile perception. In: 2011 IEEE World haptics conference (WHC), IEEE, New York, pp 621–626
156. Tang H, Beebe DJ (1998) A microfabricated electrostatic haptic display for persons with visual impairments. *IEEE Trans Rehabil Eng* 6(3):241–248
157. Taylor MM, Lederman SJ (1975) Tactile roughness of grooved surfaces: a model and the effect of friction. *Atten Percept Psychophys* 17(1):23–36
158. Terekhov AV, Hayward V (2011) Minimal adhesion surface area in tangentially loaded digital contacts. *J Biomech* 44(13):2508–2510
159. Tomlinson SE, Lewis R, Carré MJ (2009) The effect of normal force and roughness on friction in human finger contact. *Wear* 267(5–8):1311–1318. 17th international conference on wear of materials
160. Tomlinson SE, Carré MJ, Lewis R, Franklin SE (2011) Human finger contact with small, triangular ridged surfaces. *Wear* 271(9–10):2346–2353. 18th international conference on wear of materials
161. Tomlinson SE, Lewis R, Liu X, Texier C, Carré MJ (2011) Understanding the friction mechanisms between the human finger and flat contacting surfaces in moist conditions. *Tribol Lett* 41:283–294
162. Tretiakoff O, Tretiakoff A (1977) Electromechanical transducer for relief display panel. Google patents. US patent 4,044,350
163. Van Den Doel K, Pai DK (1998) The sounds of physical shapes. *Presence* 7(4):382–395
164. Van Den Doel K, Kry PG, Pai DK (2001) FoleyAutomatic: physically-based sound effects for interactive simulation and animation. In: Proceedings of the 28th annual conference on computer graphics and interactive techniques, ACM, New York, pp 537–544
165. Van Doren CL (1989) A model of spatiotemporal tactile sensitivity linking psychophysics to tissue mechanics. *J Acoust Soc Am* 85(5):2065–2080
166. Van Doren CL (1990) The effects of a surround on vibrotactile thresholds: evidence for spatial and temporal independence in the non-pacinian *i* (np *i*) channel. *J Acoust Soc Am* 87:2655
167. Verrillo RT (1962) Investigation of some parameters of the cutaneous threshold for vibration. *J Acoust Soc Am* 34:1768–1773
168. Verrillo RT (1963) Effect of contactor area on the vibrotactile threshold. *J Acoust Soc Am* 35:1962–1966
169. Verrillo RT, Bolanowski Jr SJ (1986) The effects of skin temperature on the psychophysical responses to vibration on glabrous and hairy skin. *J Acoust Soc Am* 80:528
170. Verrillo RT, Fraioli AJ, Smith RL (1969) Sensation magnitude of vibrotactile stimuli. *Atten Percept Psychophys* 6(6):366–372
171. Visell Y, Cooperstock JR (2010) Design of a vibrotactile display via a rigid surface. In: 2010 IEEE haptics symposium, pp 133–140
172. Wang Q, Hayward V (2007) In vivo biomechanics of the fingerpad skin under local tangential traction. *J Biomech* 40(4):851–860
173. Wang Q, Hayward V (2008) Tactile synthesis and perceptual inverse problems seen from the viewpoint of contact mechanics. *ACM Trans Appl Percept* 5(2):7
174. Warman PH, Ennos AR (2009) Fingerprints are unlikely to increase the friction of primate fingerpads. *J Exp Biol* 212:2016–2022
175. Watanabe T, Fukui S (1995) A method for controlling tactile sensation of surface roughness using ultrasonic vibration. In: Proceedings of the 1995 IEEE international conference on robotics and automation, vol 1, IEEE, New York, pp 1134–1139

176. Westling G, Johansson RS (1987) Responses in glabrous skin mechanoreceptors during precision grip in humans. *Exp Brain Res* 66(1):128–140
177. Wettels N, Santos VJ, Johansson RS, Loeb GE (2008) Biomimetic tactile sensor array. *Adv Robot* 22(8):829–849
178. Winfield L, Glassmire J, Colgate JE, Peshkin M (2007) T-PaD: tactile pattern display through variable friction reduction. In: *World haptics 2007*, pp 421–426
179. Witney AG, Wing A, Thonnard JL, Smith AM (2004) The cutaneous contribution to adaptive precision grip. *Trends Neurosci* 27(10):637–643
180. Wu JZ, Welcome DE, Krajnak K, Dong RG (2007) Finite element analysis of the penetrations of shear and normal vibrations into the soft tissues in a fingertip. *Med Eng Phys* 29(6):718–727
181. Yamamoto A, Nagasawa S, Yamamoto H, Higuchi T (2006) Electrostatic tactile display with thin film slider and its application to tactile telepresentation systems. *IEEE Trans Vis Comput Graph* 12(2):168–177
182. Yang TH, Pyo D, Kim SY, Cho YJ, Bae YD, Lee YM, Lee JS, Lee EH, Kwon DS (2011) A new subminiature impact actuator for mobile devices. In: *2011 IEEE World haptics conference (WHC)*, IEEE, New York, pp 95–100
183. Yao HY, Hayward V (2006) An experiment on length perception with a virtual rolling stone. In: *Proceedings of Eurohaptics*, pp 325–330
184. Yao HY, Hayward V (2010) Design and analysis of a recoil-type vibrotactile transducer. *J Acoust Soc Am* 128:619
185. Yoshioka T, Bensmaia SJ, Craig JC, Hsiao SS (2007) Texture perception through direct and indirect touch: an analysis of perceptual space for tactile textures in two modes of exploration. *Somatosens Motor Res* 24(1–2):53–70
186. Yousef H, Boukallel M, Althoefer K (2011) Tactile sensing for dexterous in-hand manipulation in robotics—a review. *Sens Actuators A, Phys*. doi:[10.1016/j.sna.2011.02.038](https://doi.org/10.1016/j.sna.2011.02.038)
187. Ziat M, Hayward V, Chapman CE, Ernst MO, Lenay C (2010) Tactile suppression of displacement. *Exp Brain Res* 206(3):299–310

Reproduction of Tactual Textures
Transducers, Mechanics and Signal Encoding
Wiertlewski, M.
2013, XIV, 133 p., Hardcover
ISBN: 978-1-4471-4840-1